



**STUDY OF THE PREPARATION AND  
CHARACTERIZATION OF ACTIVATED CARBON  
FROM *COCOS NUCIFERA L.* (COCONUT) HUSKS  
AND *MUSA PARADISIACA* (BANANA) PEEL**

by

**NUR IZZATI BINTI MOHAMAD SHUKRI**

A report submitted in fulfillment of the requirements for the degree of  
Bachelor of Applied Science (Materials Technology) with Honours

**FACULTY OF EARTH SCIENCE  
UNIVERSITI MALAYSIA KELANTAN**

2017

## DECLARATION

I declare that this thesis entitled “Study of The Preparation and Characterization of Activated Carbon from *Cocos Nucifera L.* (Coconut) Husks and *Musa Paradisiaca* (Banana) Peel” is the result of my own research except as cited in the references. The thesis has not been accepted for any degree and is not concurrently submitted in candidature of any other degree.

Signature : \_\_\_\_\_

Name : \_\_\_\_\_

Date : \_\_\_\_\_

UNIVERSITI  
MALAYSIA  
KELANTAN

## ACKNOWLEDGEMENT

Hereby, I am very grateful to ALLAH S.W.T the most gracious and the most merciful for this strength and patience to accomplished my Final Year Project (FYP). First and foremost, my sincere respect and appreciation goes to my supervisor Mr Nor Hakim Bin Abdullah for his full contribution and endless support and guidance during the entire duration of my research work or else this research will not be possible. Not to forget, my co-supervisor Dr Muhammad Azwadi Bin Sulaiman for his valuable knowledge regarding my research work.

I would also like to express this appreciation to all of the laboratory assistants which directly involved during my research work. My deepest thankful goes to Mr Fadhli, the chief laboratory assistant for Materials Technology because of his constant assist and supervision regarding laboratory matter.

The most essential thanks, I dedicated to my parents Mohd Shukri Bin Awang Noh and Noraini Bt Ismail which always be by my side giving advice, mentally and physically support and helping me in each aspects in my life.

More than that, my special gratitude I wish to express is to my entire beloved friends especially under the same supervisor which are Izzaty Bt Inu and Suhaiza Bt Abdullah for endlessly giving continuous support to me. Also my other friends that involve directly and indirectly with my research work.

NUR IZZATI BINTI MOHAMAD SHUKRI

## ABSTRACT

The main purpose of this work is to produce activated carbon from local agricultural waste by-product such as *Cocos Nucifera L.* (coconut) husks and *Musa Paradisiaca* (banana) peel. It will be synthesized through two (2) different methods which are carbonization and activation process. Coconut husks and banana peel will be carbonized in a furnace at temperature of 300°C. Then the charcoal produce will be activated with two (2) chemicals such as phosphoric acid and sodium hydroxide to investigate the elements and functional groups. More acidic condition is assume to produce larger porosity and surface area of activated carbon. Then the activated carbon produce will be analysed using several machines such as Fourier Transformation Infra-Red (Attenuated Total Reflectance) FTIR (ATR) and X-Ray Diffraction (XRD).



UNIVERSITI  
MALAYSIA  
KELANTAN

## ABSTRAK

Tujuan utama projek penyelidikan ini adalah untuk menghasilkan karbon teraktif daripada sumber terpakai agrikultur tempatan seperti sabut kelapa dan juga kulit pisang. Kedua-dua bahan ini akan dihasilkan dengan cara sintesis menggunakan dua (2) kaedah berbeza seperti proses karbonisasi dan pengaktifan. Sabut kelapa dan kulit pisang akan dikarbonisasikan di dalam relau pembakar pada suhu 300°C. Kemudian, arang akan terhasil dan ianya akan diaktifkan dengan menggunakan dua (2) bahan kimia berbeza seperti Asid Fosforik dan Natrium Hidroksida untuk mengkaji struktur liang and luas permukaan. Semakin berasid sesuatu bahan kimia yang diuji ke atas karbon teraktif, maka semakin tinggi liang and luas permukaan. Seterusnya, karbon teraktif akan dianalisis menggunakan beberapa mesin seperti *Fourier Transformation Infra-Red (Attenuated Total Reflectance) (FTIR – ATR)* dan *X-Ray Diffraction (XRD)*.



UNIVERSITI  
MALAYSIA  
KELANTAN

## TABLE OF CONTENTS

	<b>PAGE</b>
DECLARATION	
ACKNOWLEDGEMENT	ii
ABSTRACT	iii
ABSTRAK	iv
TABLE OF CONTENTS	v
LIST OF TABLES	viii
LIST OF FIGURES	ix
LIST OF ABBREVIATIONS	xi
LIST OF SYMBOLS	xii
<b>CHAPTER 1 : INTRODUCTION</b>	
1.1 Background of Study	1
1.2 Problem Statement	2
1.3 Objectives	3
<b>CHAPTER 2 : LITERATURE REVIEW</b>	
2.1 Coconut Tree ( <i>Cocos Nucifera L.</i> )	4
2.2 Banana ( <i>Musa Paradisiaca</i> ) Peel	5
2.3 Activated Carbon	5
2.4 Properties of Activated Carbon	6
2.5 Advantages of Activated Carbon	7
2.6 Classification of Activated Carbon	7
2.7 Structure of Activated Carbon	8
2.8 Characterization of Activated Carbon	8
2.8.1 X-Ray Diffraction	9
2.8.2 Fourier Transformation Infra-Red (Attenuated Total Reflectance)	9

2.9 Parameters for Activated Carbon Preparation	10
2.9.1 Chemical Agents for Activation Process	10
2.9.2 Mass Ratio of Activation Agent to Coconut Husks and Banana Peel	10
<b>CHAPTER 3 : MATERIAL AND METHOD</b>	
3.1 Materials	11
3.2 Preparation of Activated Carbon Coconut Husks ( <i>Cocos Nucifera</i> <i>L.</i> ) and Banana ( <i>Musa Paradisiaca</i> ) Peel	13
3.2.1 Carbonization Process of Coconut Husks ( <i>Cocos Nucifera</i> <i>L.</i> ) and Banana ( <i>Musa Paradisiaca</i> ) Peel	13
3.2.2 Activation Process Using Phosphoric Acid	17
3.2.3 Activation Process Using Sodium Hydroxide	17
<b>CHAPTER 4 : RESULTS AND DISCUSSION</b>	
4.1 Overview	24
4.2 Weight of activated carbon before and after activation process using $H_3PO_4$ and NaOH	24
4.2.1 Effects of activating agents to the weight of activated carbon	25
4.2.2 Effects of carbonization process to the weight of activated carbon	27
4.3 Weight loss of activated carbon after activation process using $H_3PO_4$ and NaOH	28
4.3.1 Weight loss of coconut husks activated carbon soaked with $H_3PO_4$	28
4.3.2 Weight loss of banana peel activated carbon soaked with $H_3PO_4$	28
4.3.3 Weight loss of coconut husks activated carbon soaked with NaOH	29
4.3.4 Weight loss of banana peel activated carbon soaked with NaOH	29

4.4	FTIR (ATR) spectral analysis	30
4.4.1	FTIR (ATR) spectral analysis for banana peel activated carbon impregnated with NaOH	30
4.4.2	FTIR (ATR) spectral analysis for coconut husks activated carbon impregnated with NaOH	34
4.4.3	FTIR (ATR) spectral analysis for banana peel activated carbon impregnated with H <sub>3</sub> PO <sub>4</sub>	39
4.4.4	FTIR (ATR) spectral analysis for coconut husks activated carbon impregnated with H <sub>3</sub> PO <sub>4</sub>	43
4.5	Phase identification of XRD analysis	46
4.5.1	Phase identification using XRD for banana peel activated carbon impregnated with NaOH	46
4.5.2	Phase identification using XRD for coconut husks activated carbon impregnated with NaOH	48
4.5.3	Phase identification using XRD for banana peel activated carbon impregnated with H <sub>3</sub> PO <sub>4</sub>	49
4.5.4	Phase identification using XRD for coconut husks activated carbon impregnated with H <sub>3</sub> PO <sub>4</sub>	51
<b>CHAPTER 5 : CONCLUSION</b>		
5.1	Conclusion	52
5.2	Recommendation	52
<b>REFERENCES</b>		53

UNIVERSITI  
MALAYSIA  
KELANTAN



## LIST OF TABLES

3.1	Terms used in the study	23
4.1	Weight loss of coconut husks activated carbon during activation process using $H_3PO_4$	28
4.2	Weight loss of banana peel activated carbon during activation process using $H_3PO_4$	28
4.3	Weight loss of coconut husks activated carbon during activation process using NaOH	29
4.4	Weight loss of banana peel activated carbon during activation process using NaOH	29

## LIST OF FIGURES

FIGURE		PAGE
3.1	Sodium Hydroxide (NaOH) in pellets form	11
3.2	Deionized water used to filter the pH of activated carbon after activation process using chemicals	11
3.3	Experimental process for coconut husks and banana peel activated carbon	12
3.4	Coconut husks were cut into smaller pieces	13
3.5	Drying process of coconut husks in oven	14
3.6	Coconut husks powder after carbonization process	14
3.7	Schematic diagram of pre-treatment and carbonization process of coconut husks	15
3.8	Schematic diagram of pre-treatment and carbonization process of banana peel	16
3.9	Filtration process of coconut husks and banana peel activated carbon	18
3.10	Schematic diagram activation process of coconut husks using $H_3PO_4$	19
3.11	Schematic diagram activation process of banana peel using $H_3PO_4$	20
3.12	Schematic diagram activation process of coconut husks using NaOH	21
3.13	Schematic diagram activation process of banana peel using NaOH	22
4.1	Activation process for BPAC 5%, 10% and 15% $H_3PO_4$	26
4.2	Activation process for BPAC 5%, 10% and 15% NaOH	26
4.3	FTIR (ATR) spectra of banana peel activated carbon (BPAC)	30
4.4	Structural formula for aliphatic primary amines	31
4.5	Molecular formula for aliphatic nitro compound	32

4.6	FTIR (ATR) spectra of coconut husks activated carbon (CHAC)	34
4.7	Peak showing the existence of potassium acetate at range $1577\text{ cm}^{-1}$ to $1417\text{ cm}^{-1}$ by asymmetric and symmetric stretching of $\text{CO}_2$ group	36
4.8	Peak showing the existence of sodium propionate at range $1565\text{ cm}^{-1}$ to $1426\text{ cm}^{-1}$ by asymmetric and symmetric stretching	36
4.9	Molecular formula of 2-amino-2-ethyl-1,3-propanediol	38
4.10	Molecular formula of ammonium acetate	38
4.11	FTIR (ATR) of spectra of banana peel activated carbon (BPAC)	39
4.12	Bent molecular formula for nitrite ion ( $\text{NO}_2^-$ )	40
4.13	Sharp “V” shape represent the functional group of alumina silicates	42
4.14	FTIR (ATR) spectra of coconut husks activated carbon (CHAC)	43
4.15	Structural formula for aliphatic primary amines	44
4.16	Structural formula for inorganic nitrites	44
4.17	XRD pattern of banana peel activated carbon (BPAC) impregnated with NaOH	46
4.18	XRD pattern of coconut husks activated carbon (CHAC) impregnated with NaOH	48
4.19	XRD pattern of banana peel activated carbon (BPAC) impregnated with $\text{H}_3\text{PO}_4$	49
4.20	XRD pattern of coconut husks activated carbon (CHAC) impregnated with $\text{H}_3\text{PO}_4$	51

## LIST OF ABBREVIATIONS

AC	Activated Carbon
CH	Coconut Husks
BP	Banana Peel
NaOH	Sodium Hydroxide
H <sub>3</sub> PO <sub>4</sub>	Phosphoric Acid
CHAC	Coconut Husks Activated Carbon
BPAC	Banana Peel Activated Carbon
FTIR (ATR)	Fourier Transformation Infra-red (Attenuated Total Reflectance)
XRD	X-Ray Diffraction
<i>et al.</i> ,	<i>(et alia)</i> : and others

## LIST OF SYMBOLS

$^{\circ}\text{C}$	Degree Celcius
$\text{Min}/\text{Min}^{-1}$	Minutes
pH	Power of Hydrogen
K	Kelvin
P	Pressure
$^{\circ}$	angle
$\theta$	Theta
$\text{m}^2/\text{gm}$	Meter Square per Gram Meter
nm	Nano Meter
$\mu\text{m}$	Micro Meter
cm	Centimetres
%	Percentages

UNIVERSITI  
MALAYSIA  
KELANTAN

## CHAPTER 1

### INTRODUCTION

#### 1.1 Background of Study

In this sophisticated and modern era, mankind activities have contributed to numerous developments through the world. These activities have become an issue where it leads to major problems in disposal and treatment of contamination and pollution.

Water is a basic need in humans' life. Human really depends on the usage of water to continue their lives. It is very crucial that human acquire clean and safe water source. But for some reasons, as mentioned before, it may be contaminated due to excessive activities of human (Getachew, Hussien, & Rao, 2014).

Abundant of technologies were introduced for example membrane technology, solvent extraction, reverse osmosis, dialysis, microbial degradation and ion exchange to overcome these serious problems but it seems to be high in many several aspects especially in economic aspects (Ali & Saeed, 2015).

Previous researchers found that adsorption by activated carbon (AC) can help in reducing the problem where the conventional AC seems to lack in various ways such as the ease of recovery, expensive, initial material which was hard to obtain and complex equipment used.

In many years, researchers have growing interest in producing AC when they found that AC can be synthesized from abundant of waste materials (Ali & Saeed, 2015). These waste materials can be utilized from waste to wealth and it is profitable and valuable for environmental issue to reduce the pollution and contamination.

The treatment of pollution using AC is noticeable technique where various of waste materials were used by earlier scientists to produce AC including the rice husks, coffee husks, banana peel, walnut shells, coconut shells and husks. For this work, AC will be yielded from coconut husks (CH) and banana peel (BP) by physical and chemical activation.

The physical activation method comprises the carbonisation process which the core point is to develop the formation of initial porosity while boost the carbon content in each of the raw materials (Mahanim *et al.*, 2011).

## 1.2 Problem Statement

AC derived from CH is not being explored widely yet by previous researchers, where the characterization of AC from CH is lacking. Many researchers were only focussed to the formation of AC from coconut shells. AC from agricultural waste by-products will be produced instead of the synthetic one because of the ease of operation and low cost compared to synthetic base. By using natural base, it helps in ash contents where the ash contents for CH is lower than other raw materials. Besides, it has higher volatility and has larger surface area.

### 1.3 Objectives

The objectives of this research are as follows:

1. To synthesis AC from agricultural waste by-products *Cocos Nucifera L.* (coconut) husks and *Musa Paradisiaca* (banana) peel by carbonization and activation process.
2. To characterize the synthesized AC from *Cocos Nucifera L.* (coconut) husks and *Musa Paradisiaca* (banana) peel.



**CHAPTER 2**  
**LITERATURE REVIEW**

**2.1 Coconut (*Cocos Nucifera L.*) Husks**

The coconut tree (*Cocos Nucifera L.*) is one of the well-known plant found in this tropical region which consists of several applications in various fields and also contain mineral, protein, amino acids, vitamins and phytohormones (Roopan & Elango, 2015). Large plantation of coconut tree can be found in Pacific Indonesia, Philippines, South Asia, East and West Africa and the Caribbean (Inegbenebor *et al.*, 2012). It gives benefit for both environment and communities. High waste generated from production based coconut husks has led to a serious problem where no specific industry utilizes and employs this waste.

Thus, it could contribute to the environmental pollutions (Latinwo & Agarry, 2015). In the coconut itself, it consists of shells (ectosperm) and husks (Inegbenebor *et al.*, 2012). Coconut husks can be carbonized more efficiently compared to its shells as it has the high flammability, it also can be utilized as charcoal briquettes with a binder like cassava, aloe, and root (Cobb *et al.*, 2012). Furthermore, it has wide applications as an efficient adsorbents for hazardous heavy metal like cadmium, lead and mercury (Roopan & Elango, 2015).

## 2.2 Banana (*Musa Paradisiaca*) Peel

Banana is a very customary fruit in the world where it is a lignocellulosic plant. In banana itself, it contains cellulose, lignin, pectin and other compound that contain functional groups for example carboxyl, hydroxyl, amino, alkoxy and carboxylic (Ali & Saeed, 2015). It can also be used as a precursor for AC formation. BP is easily available in huge quantities and low cost (Ma *et al.*, 2014).

The production of BP to form AC only require a simple set-up and equipment compared to the conventional production of AC (Pathak *et al.*, 2015). It is stated by Ma *et al.*, (2014) that AC from BP is a very effective solution for removal of cationic contaminants such as Methylene Blue dyes from water.

## 2.3 Activated Carbon

AC can be used as adsorbents within gaseous and liquid phases. Abundant of industrial sectors employ this material in their processing unit such as in food and beverages, petroleum, automobile, chemical and pharmaceutical sectors. AC can be obtained by extracting agricultural waste by-product through several processes.

AC is mentioned to be economically effective in removal of contaminants because of it is readily available and low cost since cost of commercially AC needs a lot of money (Azmi *et al.*, 2015). Based on previous research by (Nowicki *et al.*, (2015) another precursors utilized for

AC production such as phenolic resins, urea-formaldehyde resins and phenol formaldehyde resins are very unique and attractive but very costly. So, it is effective to utilize AC using natural sources.

Some carbonaceous waste that can generate AC include banana peels, coals, durian shells, egg shells, coffee husks and coconut shells and husks. All of these precursors can be discovered locally, normally in rural area. Among these precursors there are two main sources widely used in industry which are coconut shells and husks.

Coconut shells and husks are broadly used in industrial because of its low ash content, high volatility, larger surface area and thus very beneficial in environmental sustainability (Thomas *et al.*, 2015). Several countries show the interest for AC where the highest request came from developed countries such as Japan and United States of America in contrast for Africa which not interested in AC showing the least demand of AC (Nowicki *et al.*, 2015).

## **2.4 Properties of Activated Carbon**

AC contains ash which contribute to the volatile formation. In ash, it consists of mineral for instance silica, alumina, iron, magnesium and calcium. When AC is being analysed using several methods, it has various types of porosity such as flat surfaces of graphite-like materials run parallel to each other which is separated only by few nanometres.

Most researchers found that AC will have the microporous surface structure which is good to be used as an adsorber for contaminants and

pollution removal. The attribute of being the microporous surface structure will encourage any materials to interact with AC.

## **2.5 Advantages of Activated Carbon**

There are several advantages when utilizing AC for contaminants and pollutions treatment where it has high adsorption capacity for removal of impurities, it also contributes to economic aspects where the yielding of AC from agricultural waste by-product is inexpensive compared to conventional AC production.

Meanwhile the AC has low toxicity contents (Nowicki *et al.*, 2015). The sources of AC are ubiquitous where we can obtain it from rural area. Other than that, it can adsorb iodine extremely well.

## **2.6 Classification of Activated Carbon**

AC can be classified in several categories for instance, in powder form, granular form and pellet form based on their particle sizes, shapes, application, adsorption capacity, adsorption mechanism, raw materials used and the methods of activation (Lemaro Fereiti Angelo, 2012). Based on Laginhas *et al.*, (2016), spherical AC is said to be more regular and smoother surface, and contribute to pore size dispersion control over pore.

For this experiments, powder form AC by carbonization process at elevated temperatures will be studied. As stated by Lemaro Fereiti Angelo, (2012) powder AC must be less than 100 $\mu$ m in size, diameter range between

15 $\mu$ m and 25 $\mu$ m. Normally, it is made up from crushing or grinding. Then, the crushed and grinded particles will pass through sieving process. Small size of AC produced beneficial for large internal surface and small diffusion distance.

## 2.7 Structure of Activated Carbon

Micro crystallite will be formed during the carbonization process while activation process will disturb the regular bonding of causing free valence to exist and become very reactive. The process and impurities will interrupt the formation of interior vacancy. For coconut husks AC, it will exhibit extensive microporous pore. Structure of AC originally aromatic, size for oxidation lies within the cell wall (Lemaro Fereiti Angelo, 2012). Utilization of AC based from BP will be produced the mesoporous or microporous structure of AC (Ma *et al.*, 2014).

## 2.8 Characterization of Activated Carbon

The pore size and structure depend on the raw material itself (Chandra *et al.*, 2009). Pore size distribution is depending on the impregnation ratios of coconut husks to activating agents (Chandra *et al.*, 2009). Pore structure of AC can be divided into three groups which are microporous (under 2 nm), mesoporous (2-50 nm) and macro porous (above 50 nm) (Shankar, 2008). In recent years, microporous has been subdivided into two (2) very narrow pores which are ultra-microporous (until 0.8 nm) and super microporous (0.8 to 2.0 nm) (Virginia Hernandez-Montoya, 2015b).

Determination of the pore structure and pore size characteristics are observed under X-Ray Diffraction (XRD), X-Ray Fluorescence (XRF), Fourier Transformation Infra-red (FTIR) and Brunauer, Emmett and Teller (BET). By varying the activating agent to coconut husks ratio, optimum condition of large surface area of AC can be obtained. Inegbenebor *et al.*, (2012) stated that typical surface area for AC is approximately 1000 square meters per gram ( $\text{m}^2/\text{gm}$ ).

### **2.8.1 X-Ray Diffraction**

The X-ray diffraction (XRD) will be used for determination of phase identification of synthesized AC from CH using Bruker D2 Phaser. The step size is  $0.02^\circ$  and the range of  $2\theta$  angle is between  $10^\circ$  to  $90^\circ$ . DIFFRAC.EVA will be used for qualitative analysis.

### **2.8.2 Fourier Transformation Infra-red (Attenuated Total Reflectance)**

The FTIR used for detecting functional groups, to identify the structure of crystalized phases and to observe possible structural changes after activated. FTIR can detect specific bonds exist in material so it is possible to know which functionalities exists in carbon. It essentially utilized as a qualitative technique for the analysis of chemical structure of AC and may be for quantitative technique. This machinery intensively used for carbonaceous material when equipment with Fourier transform were accessible. Functional group is made by comparison with adsorption or transmission bands of organic compounds (Duran-Valle, 2015).

## 2.9 Parameters for Activated Carbon Preparation

### 2.9.1 Chemical Agents for Activation Process

Activating agent is the crucial agent during the activation process, where the function is to inhibit the formation of tar and other unnecessary products during the carbonization process.

For this experiment,  $H_3PO_4$  will be used as an activating agent as it is widely employed in large scale industries.  $H_3PO_4$  offers great environmental benefit such as ease of recovery, low energy cost and high carbon yield.

$H_3PO_4$  acts as template because of the volume occupied by  $H_3PO_4$  is identical to the micro pore volume of AC obtained. Besides that,  $H_3PO_4$  can act as catalyst to promote the bond cleavage, hydrolysis, dehydration and condensation. For basic condition, NaOH will be utilized to generate the porosity of AC (Virginia Hernandez-Montoya, 2015).

### 2.9.2 Mass Ratio of Activation Agent to Coconut Husks and Banana Peel

Mass ratio of activation agents to the CH and BP will be varied to find the optimum condition of AC surface area to act as adsorber. Complete saturation of CH and BP will be ensured to minimise the consumption of activation agents (Virginia Hernandez-Montoya, 2015). Activation agents used is dehydrated chemical that will penetrate deeply into the AC and develop the porosity. Thus it could contribute to increase the surface area of AC. In many cases before, the acidic condition of activation agents is responsible to form the larger surface area of the AC (Gratuito *et al.*, 2008).



## CHAPTER 3

### MATERIALS AND METHODS

#### 3.1 Materials

Coconut husks and banana peel were collected around Kg Gemang, Jeli Kelantan. Activation process was conducted using two types of chemical, which are NaOH and  $H_3PO_4$  for impregnation of AC during activation process. Distilled water was also used to remove all impurities, and deionized water has been utilized for the neutralization of pH after activation process by chemicals. All materials used were shown at figure below.



Figure 3.1: Sodium Hydroxide (NaOH) in pellets form



Figure 3.2: Deionized water used to filter the pH of activated carbon after activation process using chemicals



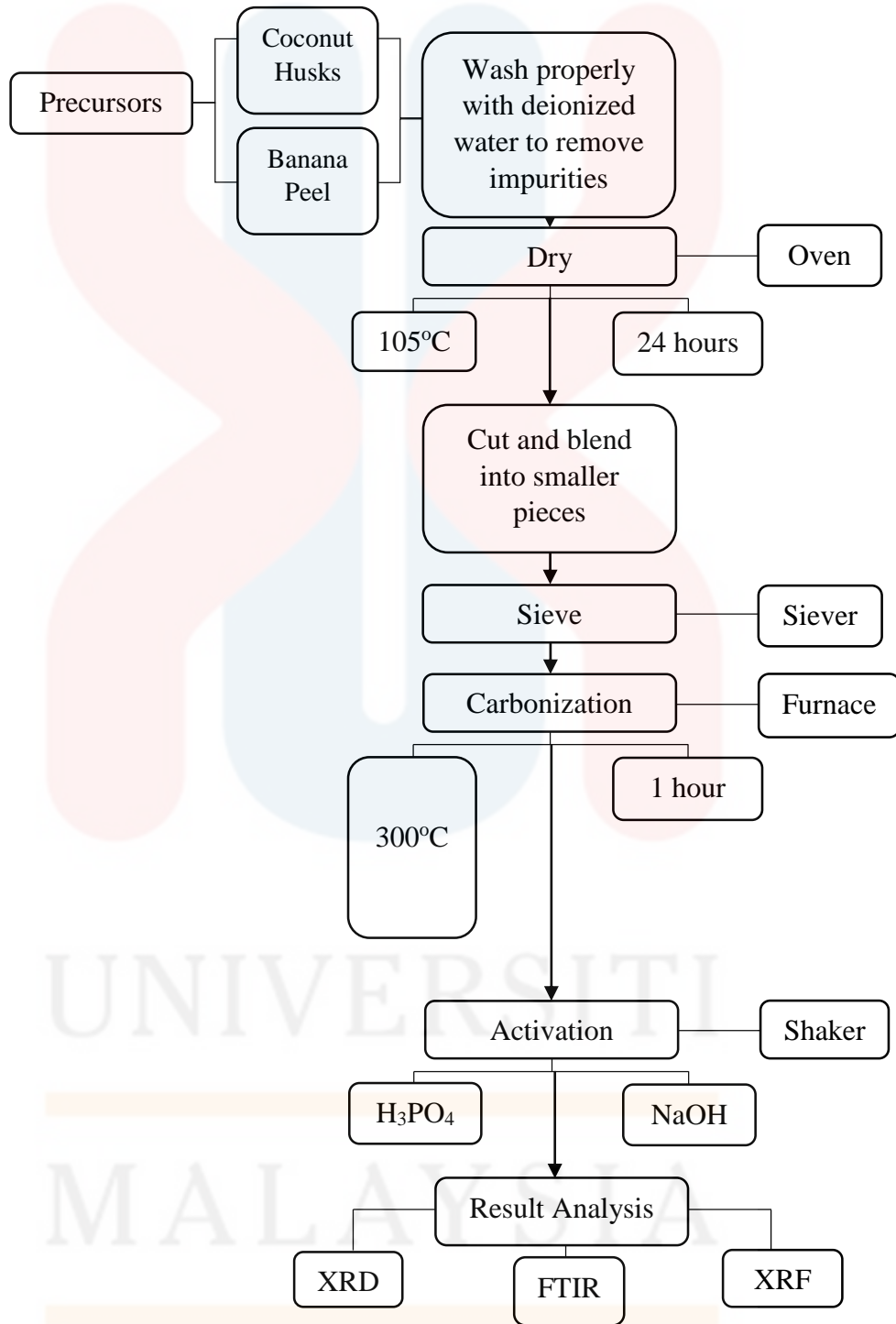


Figure 3.3: Experimental process for coconut husks and banana peel activated carbon

## 3.2 Preparation of Activated Carbon from Coconut Husks (*Cocos Nucifera L.*) and Banana (*Musa Paradisiaca*) Peel

### 3.2.1 Carbonization Process of Coconut Husks (*Cocos Nucifera L.*) and Banana (*Musa Paradisiaca*) Peel

There are two major steps in producing AC which are carbonization of the CH and followed by activation process using suitable activating agents like Sodium Hydroxide (NaOH) for basic condition and Phosphoric acid ( $H_3PO_4$ ) for acidic condition.

Firstly, the CH and BP were washed properly with deionized water to eliminate any impurities. After that, they were dried in an oven to discard the moisture content for 24 hours at 105°C. Then, they were cut into small pieces before blend and were sieved using siever to obtain the uniform size as shown at Figure 3.4 below.



Figure 3.4: Coconut husks were cut into smaller pieces



Figure 3.5: Drying process of coconut husks in oven

After drying process in oven shown in Figure 3.5 above, they were undergone carbonization process in a furnace to form powder at temperature  $300^{\circ}\text{C}$  for 1 hour for each temperature with heating rate at  $30^{\circ}\text{C min}^{-1}$ . Next, the sample were blended to form powder before sieved using siever at  $300\ \mu\text{m}$ . Figure below represents the CH powder after carbonization in furnace. Then, this powder were proceed to the next step, which was activation process using two (2) chemicals  $\text{NaOH}$  and  $\text{H}_3\text{PO}_4$ . Figures below shown the pre-treatment and carbonization process of coconut husks in Figure 3.7 and banana peel in Figure 3.8.



Figure 3.6: CH powder after carbonization process

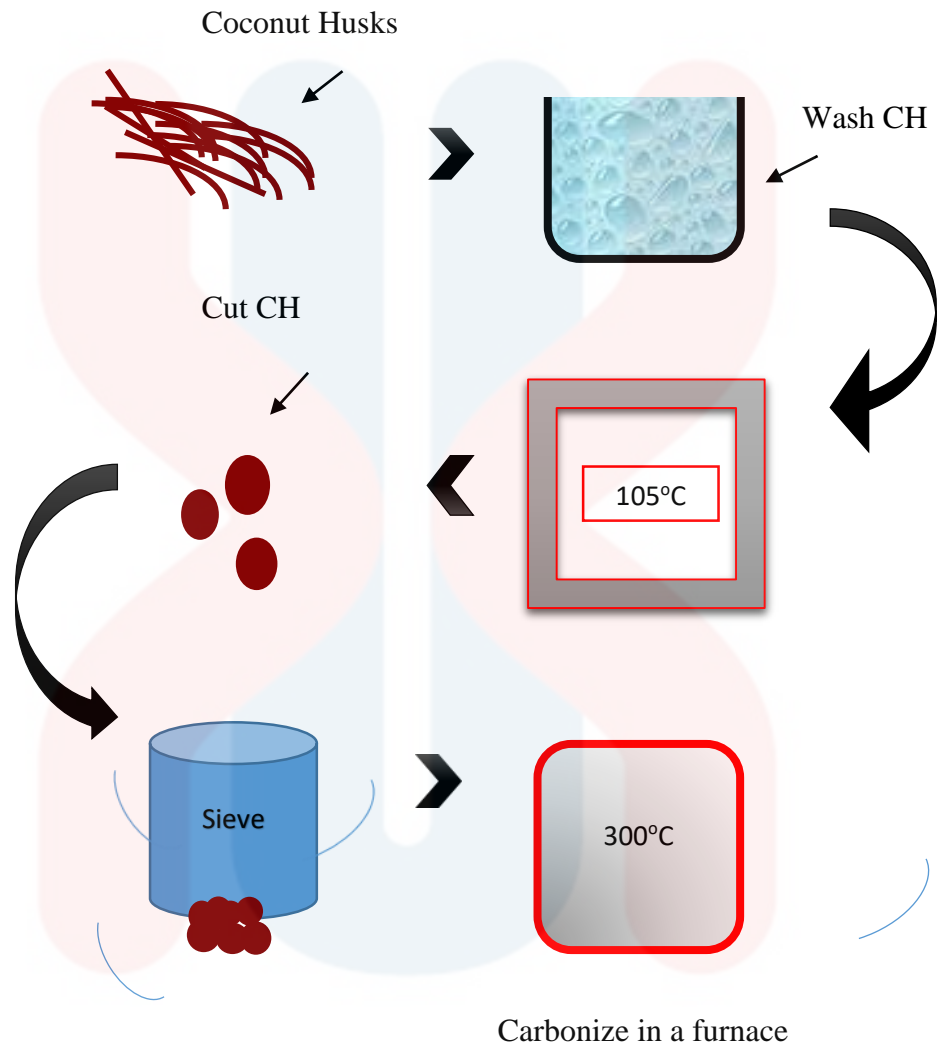


Figure 3.7: Schematic diagram of pre-treatment and carbonization process of coconut husks

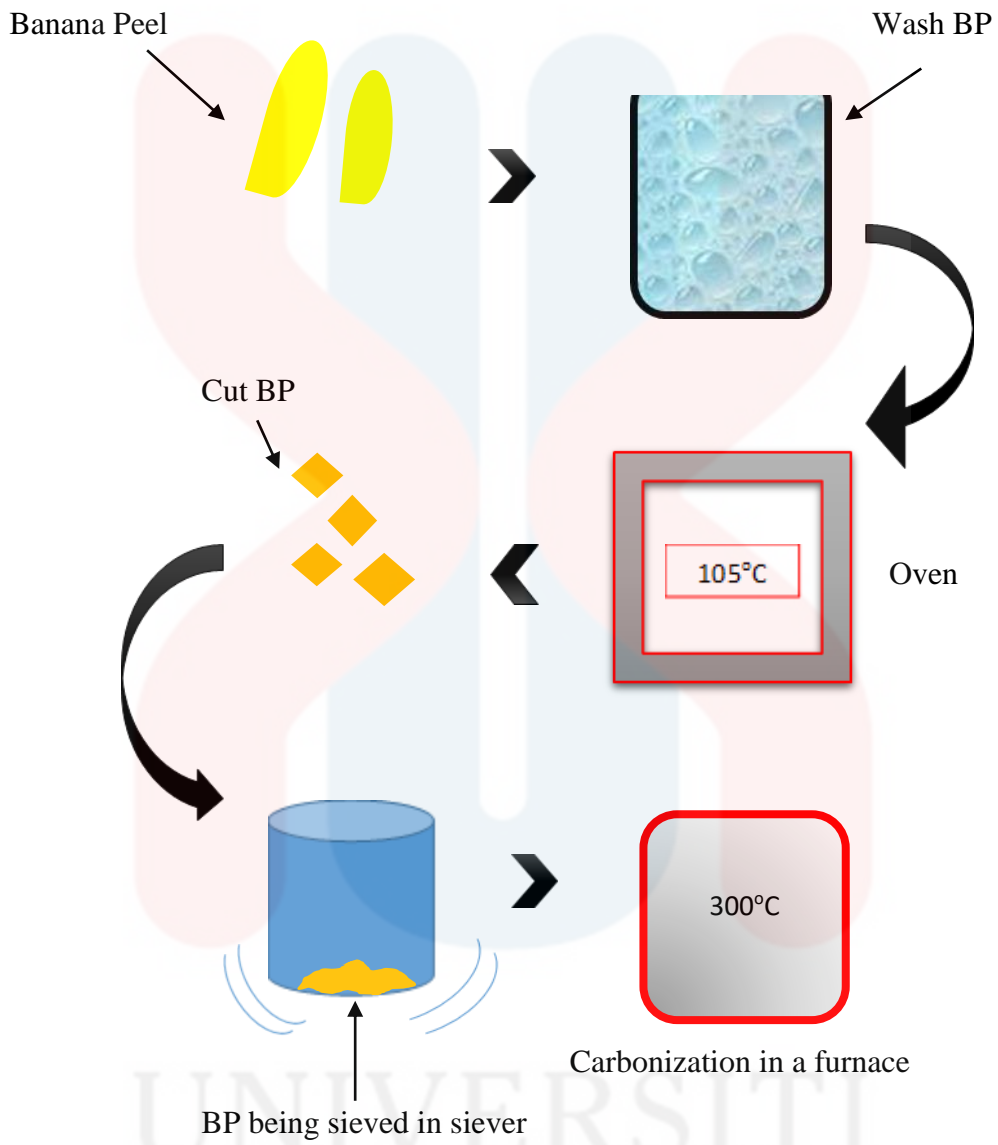


Figure 3.8: Schematic diagram of pre-treatment and carbonization process of banana peel

UNIVERSITI  
MALAYSIA  
KELANTAN

### 3.2.2 Activation Process Using Phosphoric Acid

The CH powder was activated by soaking it in 5%, 10% and 15%  $H_3PO_4$  solution. After soaking process, it was placed in an oven at  $105^\circ C$  for 24 hours to remove the moisture contents. The oven dried CH powder was kept at room temperature for 24 hours. Next, the CH was carbonized once again in a furnace at  $300^\circ C$  for 1 hour. Carbonized CH was washed with deionized water. Finally, it will be dried at  $105^\circ C$  for 3 hours in an oven and stored in zipper bag (Selvanathan & Subki, 2015). Concentrated  $H_3PO_4$  was impregnated with BP powder to activate the surface of the powder. The ratio used for the impregnation process was equal to the CH powder which are 5%, 10% and 15%  $H_3PO_4$ . From then on, BP powder was dried in an oven at  $105^\circ C$  for 24 hours to discard the water contents (Getachew *et al.*, 2014). The overall processes were illustrated in Figure 3.10 and Figure 3.11. Then, it was carbonized once again at temperature  $300^\circ C$  in furnace for 1 hour. After completed, it was washed with deionized water. Lastly, the powder was dried in oven at  $105^\circ C$  for 3 hours in oven before stored in zipper bag.

### 3.2.3 Activation Process using Sodium Hydroxide

Meanwhile for activation using NaOH, CH powder and BP powder were activated by stirring the CH powder BP powder in 5%, 10% and 15% NaOH solution. Then, they were left for 24 hours at room temperature before dried in an oven at  $105^\circ C$  for 3 hours. After that, CH powder and BP powder were carbonized in a furnace at  $300^\circ C$  for 1 hour. Next, they were filtered with deionized water as shown in figure 3.9 below to alter the pH condition to



neutral around 6-8. After, reaching the targeted pH, they were dried in oven for 105°C for 3 hours. The powders were stored zipper bag. The overall processes were illustrated in figure 3.10 and figure 3.11 for activation process of CHAC and BPAC using  $H_3PO_4$ . While figure 3.12 and 3.13 illustrate the activation process of CHAC and BPAC using NaOH.



Figure 3.9: Filtration process of CHAC and BPAC

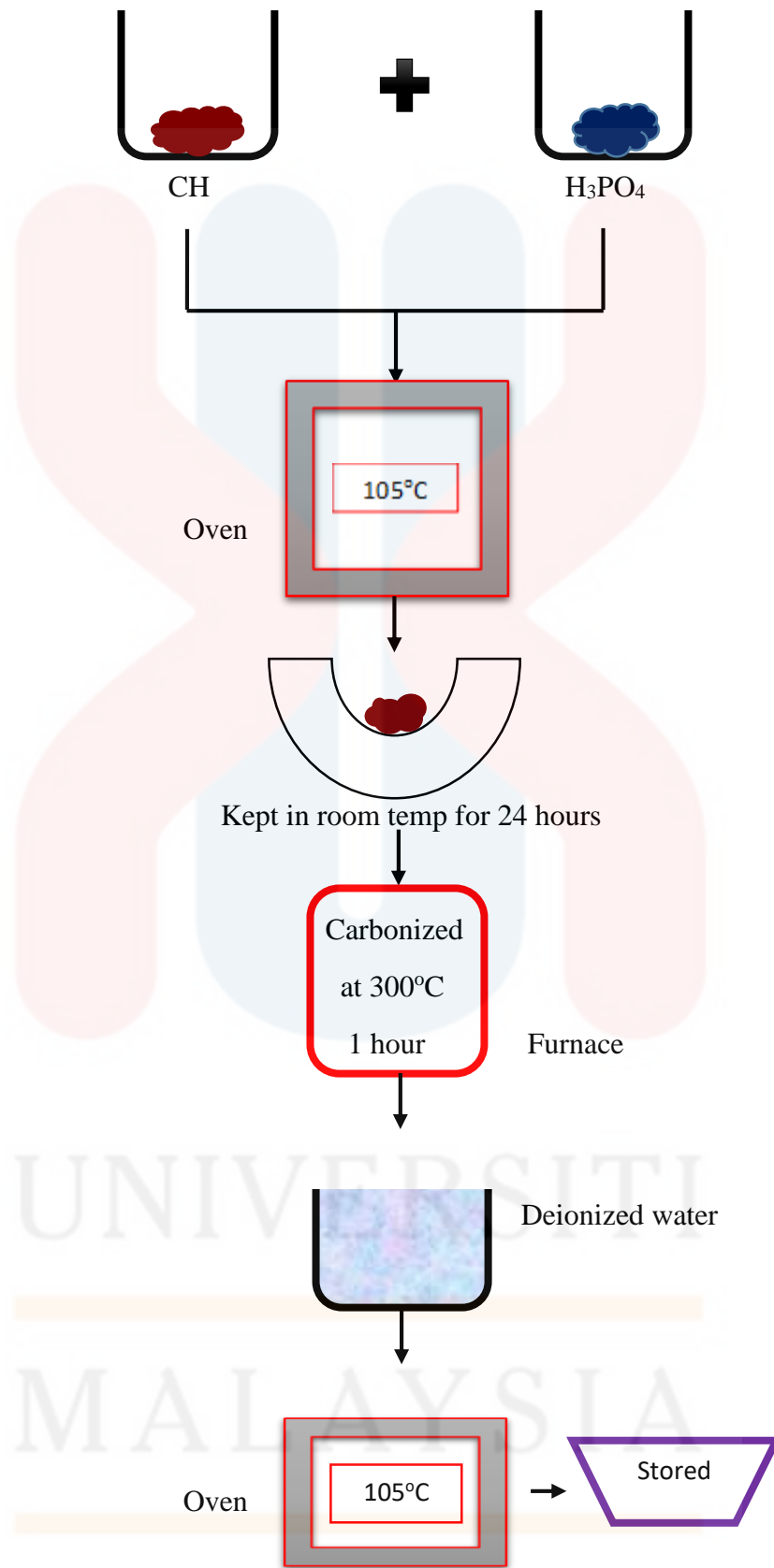


Figure 3.10: Schematic diagram activation process of CH using H<sub>3</sub>PO<sub>4</sub>



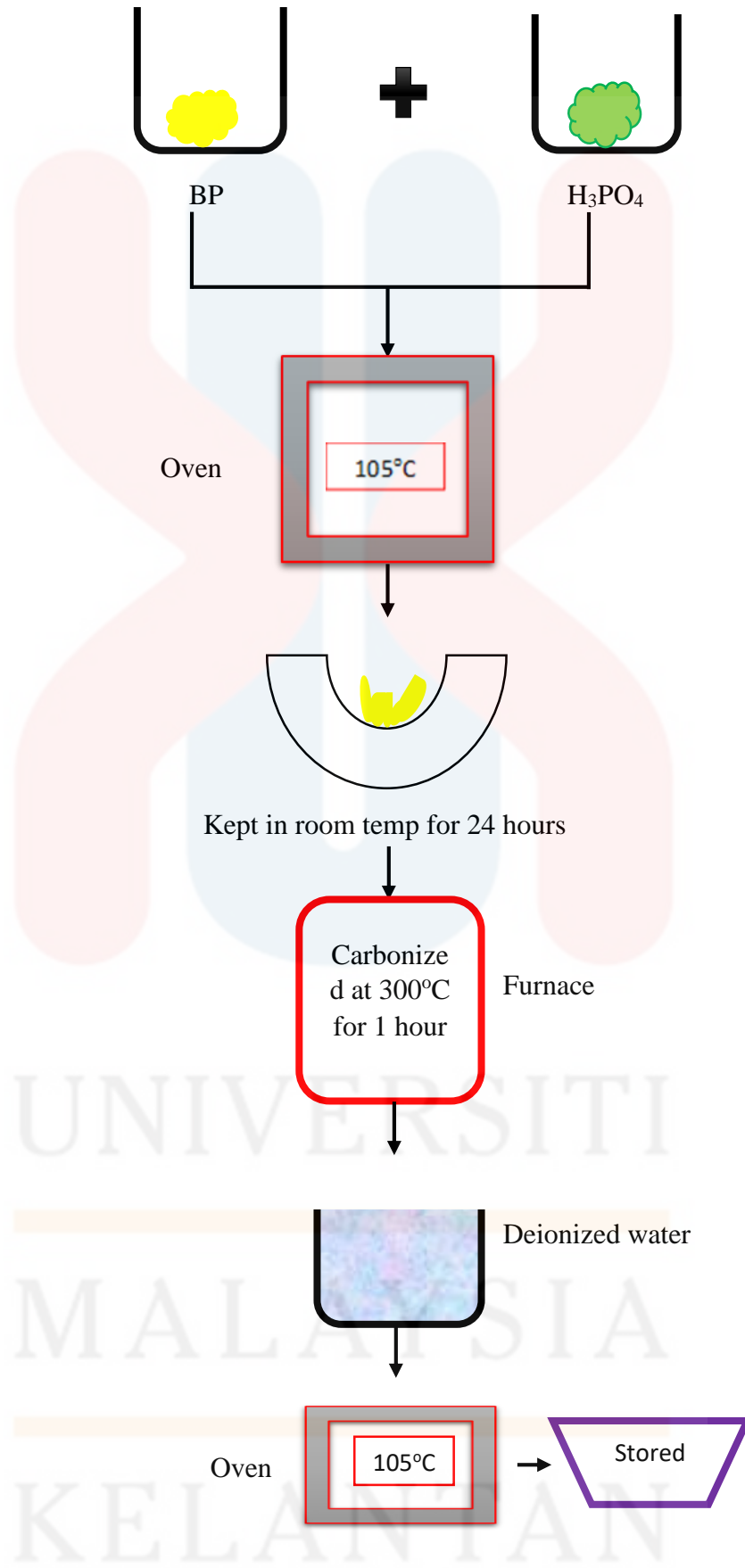


Figure 3.11: Schematic diagram activation process of BP using  $H_3PO_4$

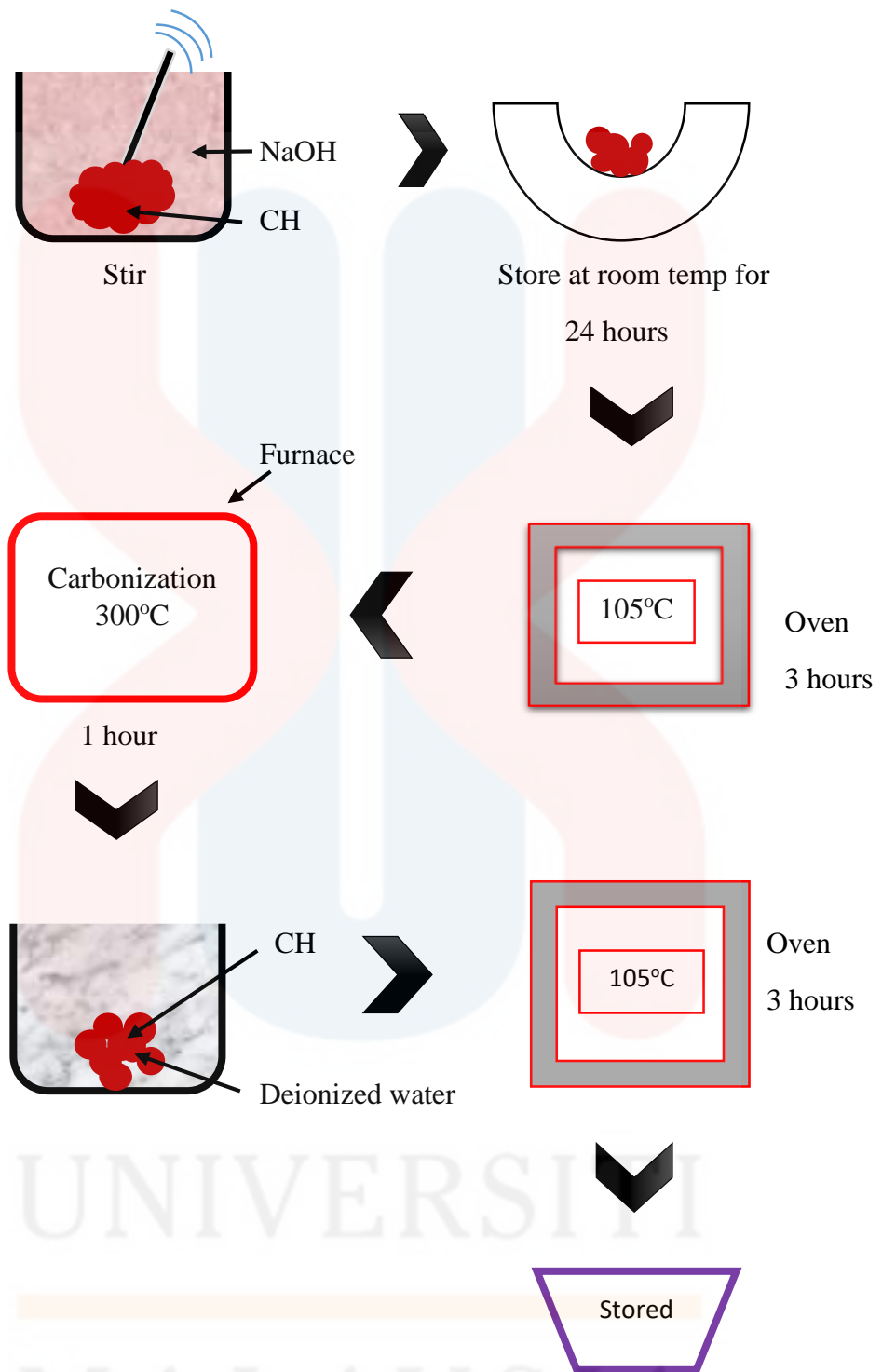


Figure 3.12: Schematic diagram activation process of CH using NaOH

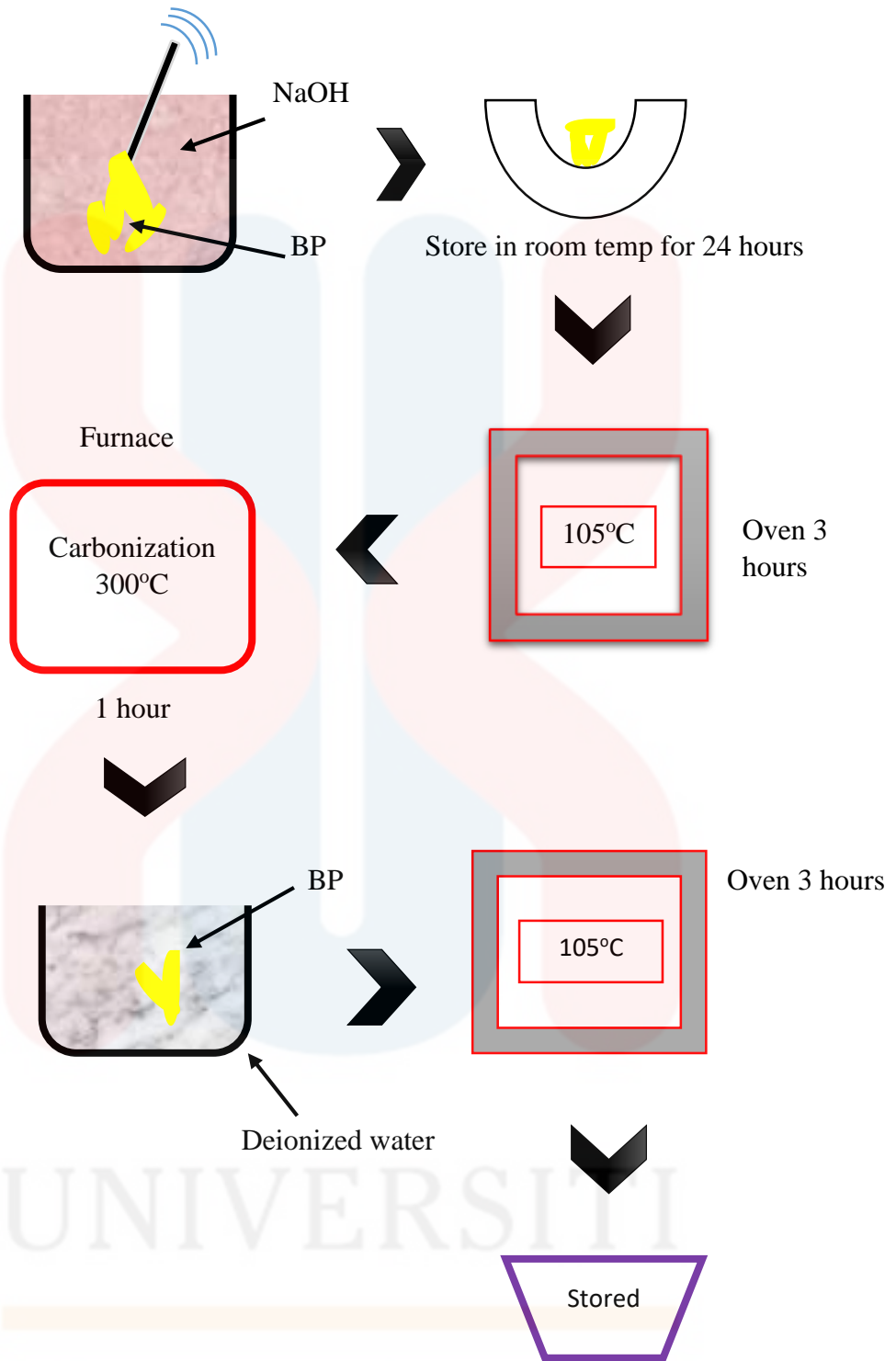


Figure 3.13: Schematic diagram activation process of BP using NaOH

Table 3.1: Terms used in this study

Activating agents used	Concentration of activating agents used (%)	CHAC	BPAC
NaOH	5	CHAC 5% NaOH	BPAC 5% NaOH
	10	CHAC 10% NaOH	BPAC 10% NaOH
	15	CHAC 15% NaOH	BPAC 15% NaOH
H <sub>3</sub> PO <sub>4</sub>	5	CHAC 5% H <sub>3</sub> PO <sub>4</sub>	BPAC 5% H <sub>3</sub> PO <sub>4</sub>
	10	CHAC 10% H <sub>3</sub> PO <sub>4</sub>	BPAC 10% H <sub>3</sub> PO <sub>4</sub>
	15	CHAC 15% H <sub>3</sub> PO <sub>4</sub>	BPAC 15% H <sub>3</sub> PO <sub>4</sub>

## CHAPTER 4

### RESULTS AND DISCUSSION

#### 4.1 Overview

This chapter discussed about the characterization of activation process for banana peel and coconut husks AC characterized by Fourier Transformation Infra-Red (FTIR) and X-Ray Diffraction (XRD). The weight loss of CHAC and BPAC were also discussed in this chapter. The peaks of all FTIR (ATR) spectrum were observed thoroughly in this part. The amorphism of CHAC and BPAC were proved by XRD analysis and were also discussed in this section.

#### 4.2 Weight of Activated Carbon Before and After Activation Process using $H_3PO_4$ and NaOH

Table below presents the overall weight loss of CHAC and BPAC after the activation process taken place. From the table, we might see the pattern of CHAC and BPAC are similar where the weight of CHAC and BPAC for acid  $H_3PO_4$  impregnation is increase from its initial weight, which is 10 g. Nevertheless, for base impregnation, it is clearly showing that the weight from initial weight, 10 g is decrease slightly for CHAC and decrease quite a lot for BPAC. The explanation of the up and down for weight initial and final for both CHAC and BPAC will be explained below.

#### 4.2.1 Effects of Activating Agents to the Weight of Activated Carbon

In chemical activation process, NaOH and H<sub>3</sub>PO<sub>4</sub> were used as agents to trigger the pores production of AC. Thus, during the chemical activation of CHAC using H<sub>3</sub>PO<sub>4</sub>, they were indicated that the initial and final weight of CHAC were altered from constant weight 10 g to 17.0 g, 24.5 g and 23.0 g for 5%, 10% and 15% H<sub>3</sub>PO<sub>4</sub> because of the residue of the impregnation of H<sub>3</sub>PO<sub>4</sub> causing the weight gain of CHAC. While for BPAC, from 10 g they did increase to 15.1 g for BPAC 5% H<sub>3</sub>PO<sub>4</sub> and for BPAC 10% and 15% H<sub>3</sub>PO<sub>4</sub>, they shared approximately the same weights 16.0 g and 16.1 g.

For NaOH, the initial and final weight showed somewhat distinct patterns from H<sub>3</sub>PO<sub>4</sub> activation where the final weight were slightly decrease to several values from initial weights, 10 g. CHAC 5% and 10% NaOH shared the same amounts where they decrease to 9.7 g and 15% NaOH decrease to 9.8 g. Dissimilar with BPAC, the results showed that the final weight became superficial. They decrease from initial weight 10 g to 4.7 g for BPAC 5%, 4.2 g for BPAC 10% and 3.2 g for BPAC 15%.

Figure 4.1 below shows the activation process for BPAC impregnated with 5%, 10% and 15% H<sub>3</sub>PO<sub>4</sub> and figure 4.2 shows BPAC impregnated with exactly the same amount of concentration for NaOH left in a room temperature for 24 hours before drying them in oven at temperature 105°C the next day.

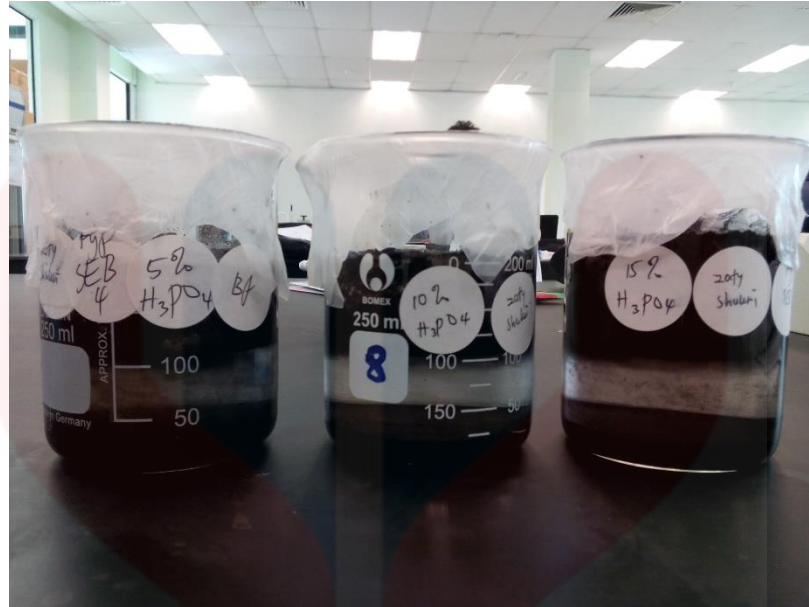


Figure 4.1: Activation process for BPAC 5%, 10% and 15% H<sub>3</sub>PO<sub>4</sub>



Figure 4.2: Activation process for BPAC 5%, 10% and 15% NaOH

KELANTAN

#### 4.2.2 Effects of Carbonization Process to the Weight of Activated Carbon

The process of carbonization once again operated after the activation by activating agents aforementioned. This process was to let the AC in its' driest condition. The water content in AC in the form of vapour needs to be discarded, and it crave a lot of energy to do so. The samples were leaved for 24 hours at room temperature to pre-dry it before carbonization process occurred in the furnace to remove all the moisture content.

This process was fulfilled by placing the AC into the furnace at temperature 300°C for 1 hour at heating rate of 30°C per minute, the partial combustion of the AC charged to the furnace and it was energy adsorbing or as well as endothermic energy reaction. The time taken for the temperature to increase was 20 min. During soaking process about 10 min, the samples were spontaneously break down to produce AC and other complex chemicals mainly hydrogen, carbon dioxide and carbon monoxide. This process occurred at temperature above 280°C and liberates energy, and it was called exothermic reaction. Another 30 min to cool off the samples.

The initial and final weight of AC was illustrated at table below where it showed declined in the weight for both CHAC and BPAC impregnated with  $H_3PO_4$  and NaOH activating agents.



### 4.3 Weight Loss of Activated Carbon after Activation Process using $H_3PO_4$ and NaOH

#### 4.3.1 Weight Loss of Coconut Husks Activated Carbon Soaked with $H_3PO_4$

Table below shows the percentage of weight loss of CHAC for initial and final weight after activation process impregnated with 5%, 10% and 15%  $H_3PO_4$ .

Table 4.1: Weight Loss of Coconut Husks Activated Carbon during Activation Process using  $H_3PO_4$

Activating Agent	Concentration (%)	Weight Initial (g)	Weight Final (g)	Percentage weight loss (%)
$H_3PO_4$	5	17.0	15.6	8.2
	10	24.5	22.4	8.6
	15	23.0	21.1	8.3

#### 4.3.2 Weight Loss of Banana Peel Activated Carbon Soaked with $H_3PO_4$

Table below shows the percentage of weight loss of BPAC for initial and final weight after activation process impregnated with 5%, 10% and 15%  $H_3PO_4$ .

Table 4.2: Weight Loss of Banana Peel Activated Carbon during Activation Process using  $H_3PO_4$

Activating Agent	Concentration (%)	Weight Initial (g)	Weight Final (g)	Percentage weight loss (%)
$H_3PO_4$	5	15.1	14.9	1.3
	10	16.0	15.2	5.0
	15	16.1	15.5	3.7

### 4.3.3 Weight Loss of Coconut Husks Activated Carbon Soaked with NaOH

Table below shows the percentage of weight loss of CHAC for initial and final weight after activation process impregnated with 5%, 10% and 15% NaOH.

Table 4.3: Weight Loss of Coconut Husks Activated Carbon during Activation Process using NaOH

Activating Agent	Concentration (%)	Weight Initial (g)	Weight Final (g)	Percentage weight loss (%)
NaOH	5	9.7	9.2	5.2
	10	9.7	9.3	4.1
	15	9.8	9.1	7.1

### 4.3.4 Weight Loss of Banana Peel Activated Carbon Soaked with NaOH

Table below shows the percentage of weight loss of BPAC for initial and final weight after activation process impregnated with 5%, 10% and 15% NaOH.

Table 4.4: Weight Loss of Banana Peel Activated Carbon during Activation using NaOH

Activating Agent	Concentration (%)	Weight Initial (g)	Weight Final (g)	Percentage of weight loss (%)
NaOH	5	4.7	3.3	29.8
	10	4.2	2.2	47.7
	15	3.2	2.8	12.5

## 4.4 FTIR (ATR) Spectral Analysis

### 4.4.1 FTIR (ATR) Spectral Analysis for Banana Peel Activated Carbon Impregnated with NaOH

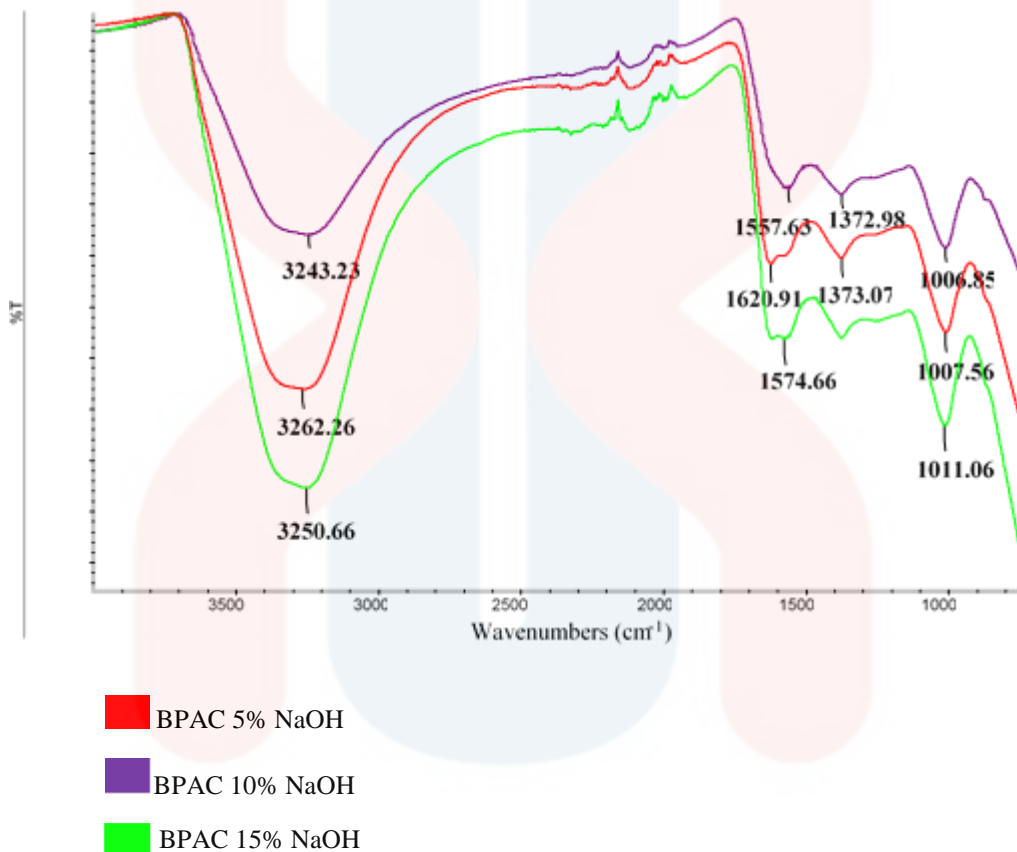


Figure 4.3: FTIR (ATR) spectra of banana peel activated carbon (BPAC)

**Figure 4.3** shows the FTIR spectral analysis results for BPAC 5%, 10% and 15% impregnated with NaOH chemical respectively. As it can be seen, from **BPAC 5% NaOH**, the adsorption peaks appearing at 3262.26 cm<sup>-1</sup>, 1620.91 cm<sup>-1</sup>, 1373.07 cm<sup>-1</sup> and 1007.56 cm<sup>-1</sup> respectively. The first peak exist at 3262.26 cm<sup>-1</sup> is alcohol or in details as the slightly elongated “U” shape assigned a primary aliphatic alcohol indicates there is OH bonding.

Second peak at  $1620.91\text{ cm}^{-1}$  presents the aliphatic primary amines group consists of single group attached to the nitrogen atom.

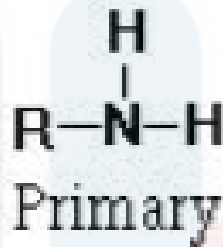


Figure 4.4: Structural formula for aliphatic primary amines

Here, the NH deformation occurred around  $1590\text{ cm}^{-1}$  to  $1650\text{ cm}^{-1}$  indicates the existence of nitrogen as the sign of basicity. While another two (2) peaks share the same functional group that is inorganic phosphates. The NH group dissipate because of the strong CH adsorption occurs around bands  $1000\text{ cm}^{-1}$  and  $550\text{ cm}^{-1}$ . Very weak peaks arise at  $1373.07\text{ cm}^{-1}$  and  $1007.56\text{ cm}^{-1}$  correlated with the inorganic phosphate group due to the P=O stretching and P-O-C bonding respectively, the existence of phosphate group at peak  $1007.56\text{ cm}^{-1}$  is due to the presence of  $\text{H}_3\text{PO}_4$  in the preparation of AC (Taylor *et al.*, 2015).

**BPAC 10% NaOH** displays the adsorption peaks at  $3243.23\text{ cm}^{-1}$ ,  $1557.63\text{ cm}^{-1}$ ,  $1372.98\text{ cm}^{-1}$  and  $1006.85\text{ cm}^{-1}$  respectively. The major functional groups in these regions present are inorganic phosphates and aliphatic primary amines. The first peak is said to be in details as primary aliphatic alcohols due to the elongated “U” shape appears, this functional group is similar with **BPAC 5% NaOH** where the OH bonding stretching occurs at this point.

Carboxylic acid appears in second peaks of this graph was indicated by the strong stretching adsorption of CO<sub>2</sub> group around the region of 1650 cm<sup>-1</sup> to 1550 cm<sup>-1</sup>. When mixing the water-soluble organic compound with NaOH, interaction between the mixtures producing always almost carboxylic acid that reacts with the NaOH solution to alter back the condition of acidic. For adsorption peaks at 1372.98 cm<sup>-1</sup>, aliphatic nitro compounds containing nitrates, nitrites and nitros appear. It has two (2) major adsorption between range of 1645 cm<sup>-1</sup> and 870 cm<sup>-1</sup> that are symmetric and asymmetric stretch, which corresponds to the strong adsorption with high frequency.

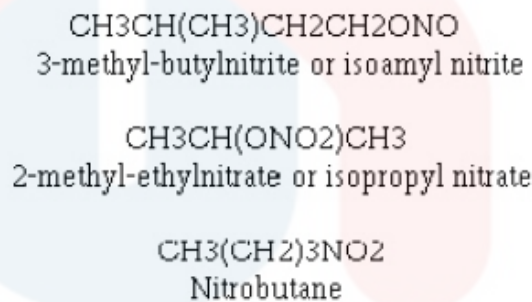


Figure 4.5: Molecular formula of aliphatic nitro compound

The last peak for *BPAC 10% NaOH*, C-SO-C adsorption occur at around 1100 cm<sup>-1</sup> to 950 cm<sup>-1</sup> is appointed as the aromatic SO compounds, basically the aromatic functional group has weak reactivity and boost extreme stability due to its aromaticity.

***BPAC 15% NaOH*** displays almost the same functional group that exist during the activation process of AC with activating chemical agents. At peaks 3250.66 cm<sup>-1</sup>, 1574.66 cm<sup>-1</sup> and 1011.06 cm<sup>-1</sup> were appointed with

inorganic phosphates, aromatic isothiocyanates, aliphatic isothiocyanates and aliphatic isocyanides. Aforementioned, for the first peak it almost always appears as primary aliphatic alcohol that exist the OH bonding are assigned by the elongated “U” shape. Then, the pattern of the graph continue by sloping the line to the second peak that occurs the C=N stretching for open chain compounds between range  $1610\text{ cm}^{-1}$  to  $1480\text{ cm}^{-1}$ . The conjugation of cyclic compounds corresponding in the regions from  $1660\text{ cm}^{-1}$  to  $1480\text{ cm}^{-1}$  respectively. A very weak peak appear at  $1011.06\text{ cm}^{-1}$ , which corresponds, to the aliphatic isocyanides being catalysed by base NaOH. R-N=C=O is the bonding appear in the region.

#### 4.4.2 FTIR (ATR) Spectral Analysis for Coconut Husks Activated Carbon Impregnated with NaOH

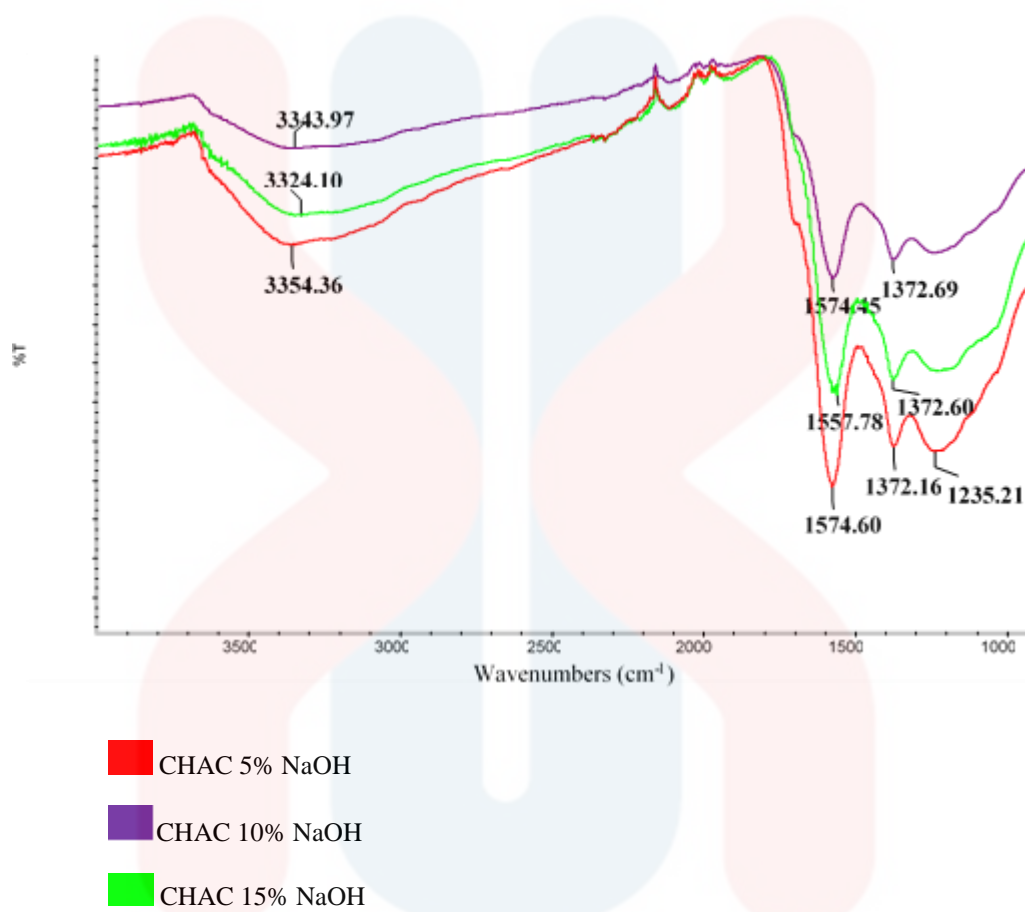


Figure 4.6: FTIR (ATR) spectra of coconut husks activated carbon (CHAC)

**Figure 4.6** displays the CHAC 5%, 10% and 15% NaOH contribute to the major existence of aliphatic carboxylic acid salts. Carboxylic acid has high boiling points even higher than alcohol, this is because of the dimer (pair of acid molecules) strongly held together by two (2) hydrogen bonds between carbonyl group, C=O and hydroxyl group, OH. This combination results in wide band adsorption in infra-red spectrum with OH stretching adsorption exists around 3100 cm<sup>-1</sup> to 2100 cm<sup>-1</sup>. Carboxylic acid is weaker acid compared to mineral acids such as H<sub>3</sub>PO<sub>4</sub>, HNO<sub>3</sub> and H<sub>2</sub>SO<sub>4</sub> but is more

acidic compared to weak organic acid such as alcohol and acetylene. Carboxylate ion presents in the carboxylic acid in aqueous solution. Aforementioned in figure 4.4, the reaction between the water soluble organic compound with cold and dilute NaOH resulting in carboxylic acid. Thus, the acid will dissolve in NaOH to be converted back to its original condition.

For peak  $3354.36\text{ cm}^{-1}$  at *CHAC 5% NaOH*, it is said to have 3-amino-1,2-propanediol representing the carboxylic acid group. The C=O group and OH group interact to each other to make the acid less vulnerable. While the OH bonding ruptures and releases  $\text{H}^+$  ion. Then *CHAC 5% NaOH* shows that potassium acetate appears as shown in Figure 4.7 below at the region  $1574.60\text{ cm}^{-1}$  showing the asymmetric stretching adsorption from  $\text{CO}_2$  group. The adsorption band around  $1700\text{ cm}^{-1}$  dissipates and is replaced by these two (2) bands. Representing the  $\text{CO}_2$  bonding is the steep V and narrow down peak pattern. Next, another peak at *CHAC 5% NaOH* contributes to the presence of cellulose acetate butyrate at peak  $1372.16\text{ cm}^{-1}$  when the nitrogen compounds are likely to adsorb strongly around  $1560\text{ cm}^{-1}$  and  $1390\text{ cm}^{-1}$ . It has higher frequency and is most extreme. The last peak gives appearance to the sodium propionate as shown in Figure 4.8 below. There is slight stretching of C-O bonding at range around  $1235.21\text{ cm}^{-1}$ .



## POTASSIUM ACETATE

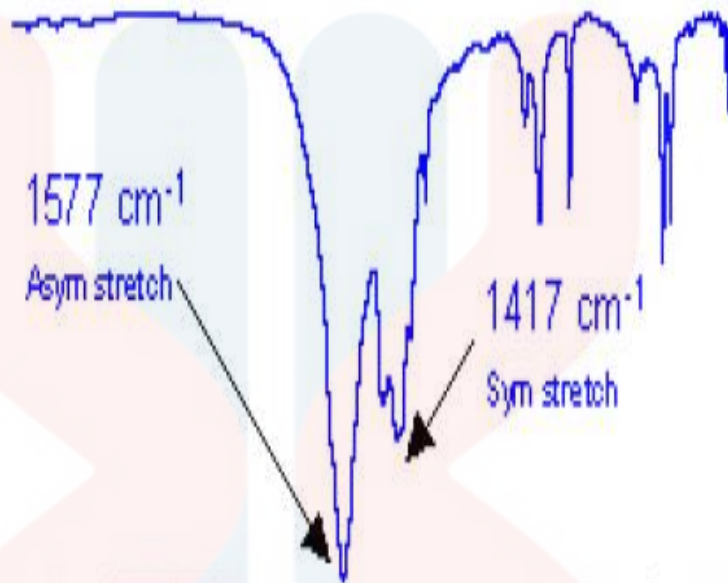


Figure 4.7: Peak showing the existence of potassium acetate at range  $1577 \text{ cm}^{-1}$  to  $1417 \text{ cm}^{-1}$  by asymmetric and symmetric stretching of  $\text{CO}_2$  group

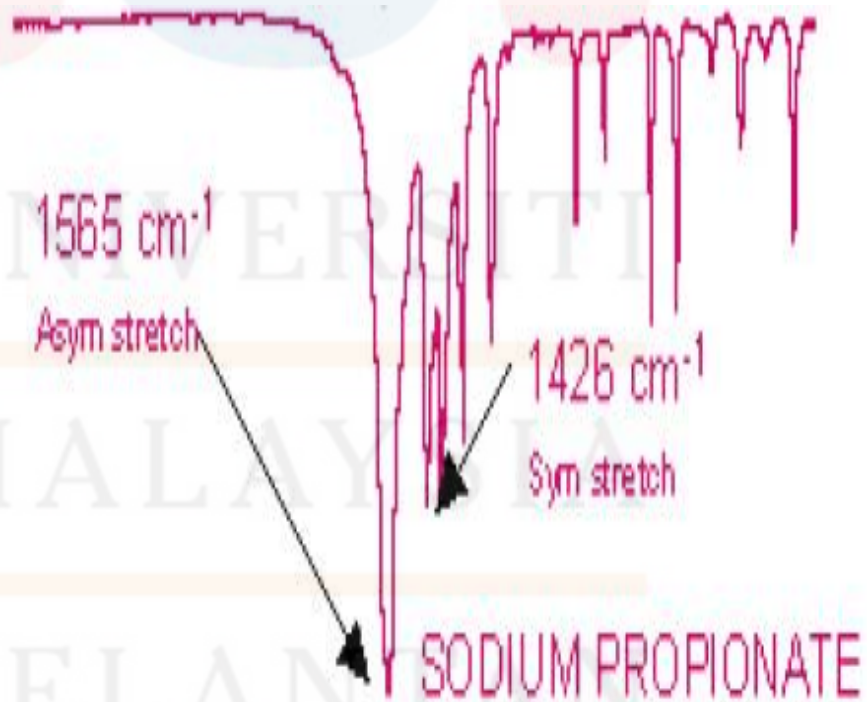


Figure 4.8: Peak showing the existence of sodium propionate at range  $1565 \text{ cm}^{-1}$  to  $1426 \text{ cm}^{-1}$  by asymmetric and symmetric stretching

**CHAC 10% NaOH**, shows the FTIR spectral analysis for the next peaks. For this figure, functional group appear is similar with **CHAC 5% NaOH** that is aliphatic carboxylic acid salts. This results in the formation of poly(ethylene vinyl alcohol) at  $3343.97\text{ cm}^{-1}$  in **CHAC 10% NaOH**. When we compare to the previous FTIR spectral analysis above, almost all peak region at range  $3600\text{ cm}^{-1}$  to  $2150\text{ cm}^{-1}$  exist because of the stretching of hydroxyl group OH bonding. Then we move to  $1574.45\text{ cm}^{-1}$  where the formation of ammonium acetate occurs through the process of asymmetric stretching from  $\text{CO}_2$  group in peaks range from  $1530\text{ cm}^{-1}$  to  $1500\text{ cm}^{-1}$  region.

While in this peak  $1372.69\text{ cm}^{-1}$ , the contribution of  $\text{CO}_2$  stretching results in poly(acrylic acid) formation. Comparison to the previous FTIR spectral at **CHAC 5% NaOH** above, there is necessary the existence of  $\text{CO}_2$  stretching around these peaks. For acid in high electronegativity, the asymmetric adsorption will shift to higher frequency.

As expected, **CHAC 15% NaOH** gives the result of aliphatic carboxylic acid salts similar with **CHAC 5%** and **10% NaOH** previously. Ketcha *et al.*, (2012) said, they almost OH stretching adsorption around  $3500\text{ cm}^{-1}$  to  $3200\text{ cm}^{-1}$  peaks where in this sample, stretching adsorption occurs at peak  $3324.10\text{ cm}^{-1}$  where the elongated “U” shape indicate the OH bonding at the nominated region producing the 2-amino-2-ethyl-1,3-propanediol in Figure 4.9 below. Thus, this also indicates that there is carboxylate ion that exists automatically due to the interaction between  $\text{CO}_2$  group.

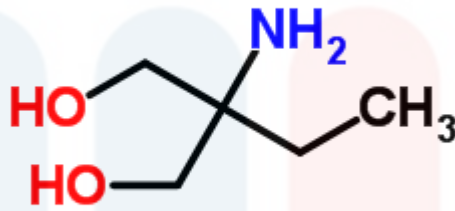


Figure 4.9: Molecular formula of 2-amino-2-ethyl-1,3-propanediol

The peak rise gradually and start to decline rapidly at  $1530\text{ cm}^{-1}$  until it reaches  $1557.78\text{ cm}^{-1}$  and eager the formation of ammonium acetate in Figure 4.10 below correlated with the stretching adsorption at  $\text{CO}_2$  group from peak  $3324.10\text{ cm}^{-1}$ . This adsorption corresponds to the asymmetric and symmetric vibration of R-COO group. After a while, it slightly increase before went down at around  $1400\text{ cm}^{-1}$  to  $1300\text{ cm}^{-1}$  which showing the presence of nitrogen compound with higher frequency and most intense.

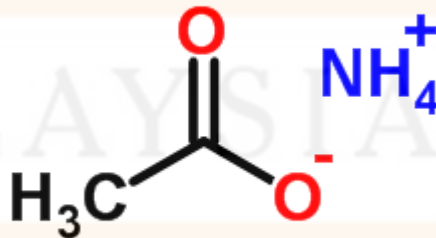


Figure 4.10: Molecular formula of ammonium acetate

#### 4.4.3 FTIR (ATR) Spectral Analysis for Banana Peel Activated Carbon Impregnated with H<sub>3</sub>PO<sub>4</sub>

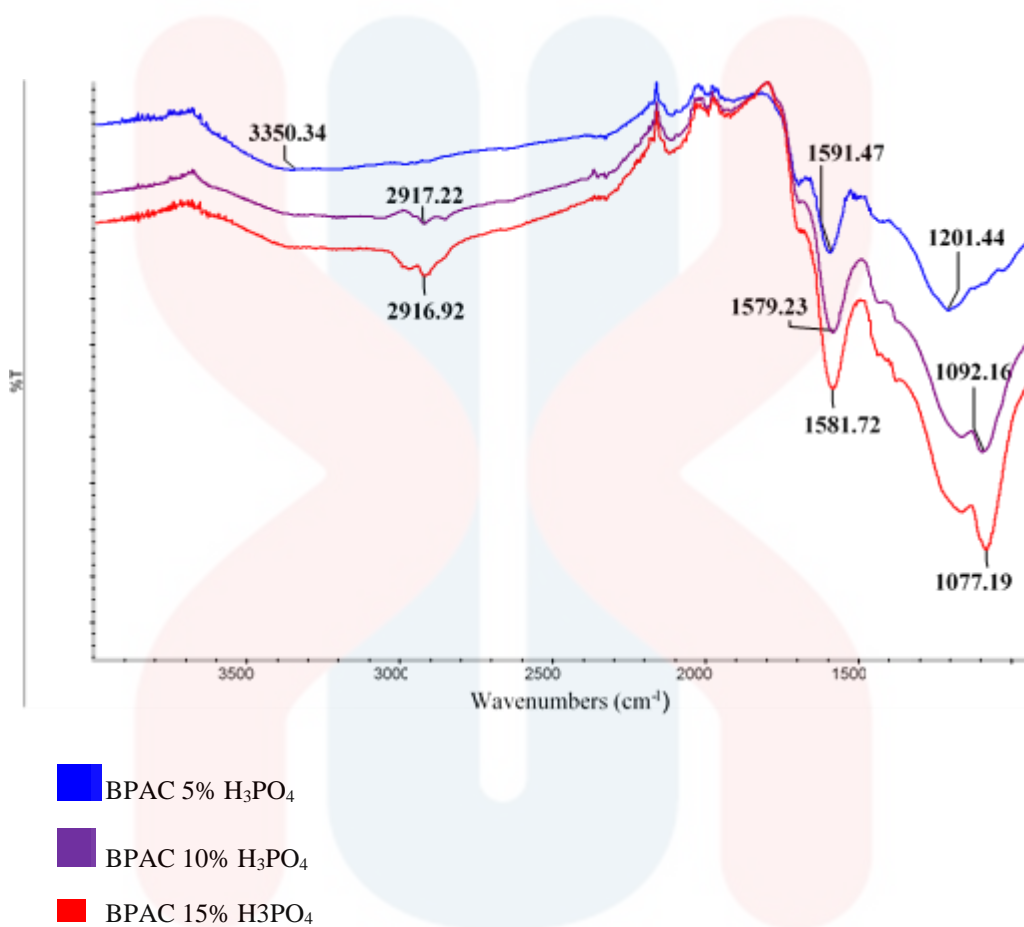


Figure 4.11: FTIR (ATR) spectra of banana peel activated carbon (BPAC)

This graph represents the BPAC impregnated with H<sub>3</sub>PO<sub>4</sub> with distinct concentration 5%, 10% and 15% respectively. Figure above shows **BPAC 5% H<sub>3</sub>PO<sub>4</sub>** which contributes to three (3) relevant peaks that are 3350.34 cm<sup>-1</sup>, 1591.47 cm<sup>-1</sup> and 1201.44 cm<sup>-1</sup>. From the graph, the presence of two (2) functional groups can be detected, that are inorganic nitrites and aliphatic amino acid salts. It has nitrous acid with general formula of HNO<sub>2</sub> and contains nitrite ion (NO<sub>2</sub><sup>-</sup>) with bent molecular formula as shown in Figure 4.12 below.

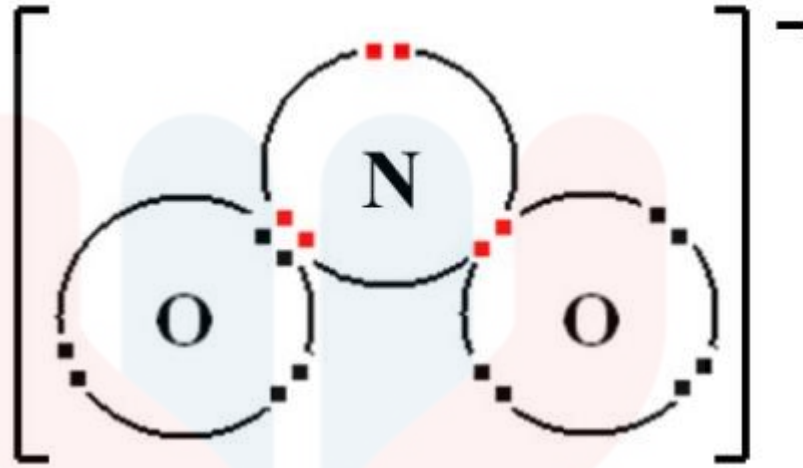


Figure 4.12: Bent molecular formula for nitrite ion (NO<sub>2</sub><sup>-</sup>)

For this sample, peak 3350.34 cm<sup>-1</sup> shows that O-H and N-H stretching occurs indicates the presence of alcohol in the sample. Also the water adsorption occurs at this peaks, almost all samples above has water adsorption at this “U” elongated shape (Ketcha *et al.*, 2012). The OH bonding appearance also contributes to the presence of carboxylic acid (COOH) group, which indicates the acidity of BPAC. At peak 1591.47 cm<sup>-1</sup> the stretching of OH and NH bonding is slowly reduce. From the previous study by Zheng & Wang (2013), it was said that around peaks 1600 cm<sup>-1</sup> to 950 cm<sup>-1</sup> the polysaccharides chain is damaged due to the temperature of 500°C is applied during carbonization process. Whilst for the last peak, observation based on the peak 1201.44 cm<sup>-1</sup> where here the stretching of weak adsorption of C-SO-C appointed in the aromatic SO compounds, as Ma *et al.*, (2014) declared in his previous study, the weak adsorption appeared around this related peak indicated the stretching adsorption of sulphate group.

Next, for **BPAC 10% H<sub>3</sub>PO<sub>4</sub>**, the peaks were likely to appear at 2917.22 cm<sup>-1</sup> that indicates the functional group of aliphatic hydrocarbon.

Here, the CH stretching adsorption occurs at around  $3000\text{ cm}^{-1}$  to  $2800\text{ cm}^{-1}$  where atoms directly attached to the aliphatic group resulting in the significant shift of atoms with higher electronegativity standard frequency to higher frequency. Ma *et al.*, (2014) stated in the previous study that stretching adsorption occur at peaks around  $2925\text{ cm}^{-1}$  to  $2854\text{ cm}^{-1}$  where the CH bonding of methylene were assigned here. While for the peak that appears at  $1579.23\text{ cm}^{-1}$  for *BPAC 10% H<sub>3</sub>PO<sub>4</sub>* and peaks  $2916.92\text{ cm}^{-1}$  and  $1581.72\text{ cm}^{-1}$  for *BPAC 15% H<sub>3</sub>PO<sub>4</sub>* share the same functional group which is aliphatic amino acid is said to be non-volatile, insoluble in non-polar solvents and soluble in water. Thus, at this peak  $1579.23\text{ cm}^{-1}$ , occur the COOH bonding correlated to the carboxylic acid which exists through the impregnation of acid resulting the carboxylate ion produced. Alumino silicates presents at the last peak,  $1092.16\text{ cm}^{-1}$  for *BPAC 10% H<sub>3</sub>PO<sub>4</sub>* and at peak  $1077.1\text{ cm}^{-1}$  for *BPAC 15% H<sub>3</sub>PO<sub>4</sub>* the steep “V” shape contributes to the association of water molecule that exists around band  $3400\text{ cm}^{-1}$  to  $1640\text{ cm}^{-1}$ , thus the collaboration with this water molecule gives rise to sharp band formation as shown in Figure 4.13 below. Basically the C-C and C-N stretching adsorption exists around peaks  $1097\text{ cm}^{-1}$  to  $1053\text{ cm}^{-1}$  respectively (Taylor *et al.*, 2015).

MALAYSIA

KELANTAN

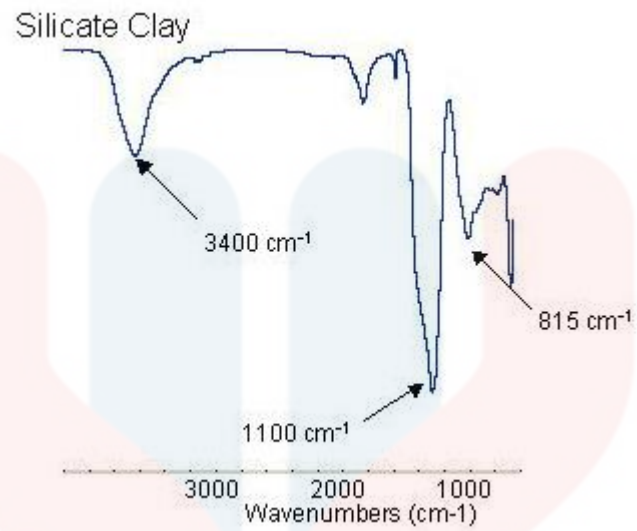


Figure 4.13: Sharp “V” shape peaks represent the functional group of alumina silicates



#### 4.4.4 Characterization of FTIR Spectral Analysis for Coconut Husks Activated Carbon Impregnated with H<sub>3</sub>PO<sub>4</sub>

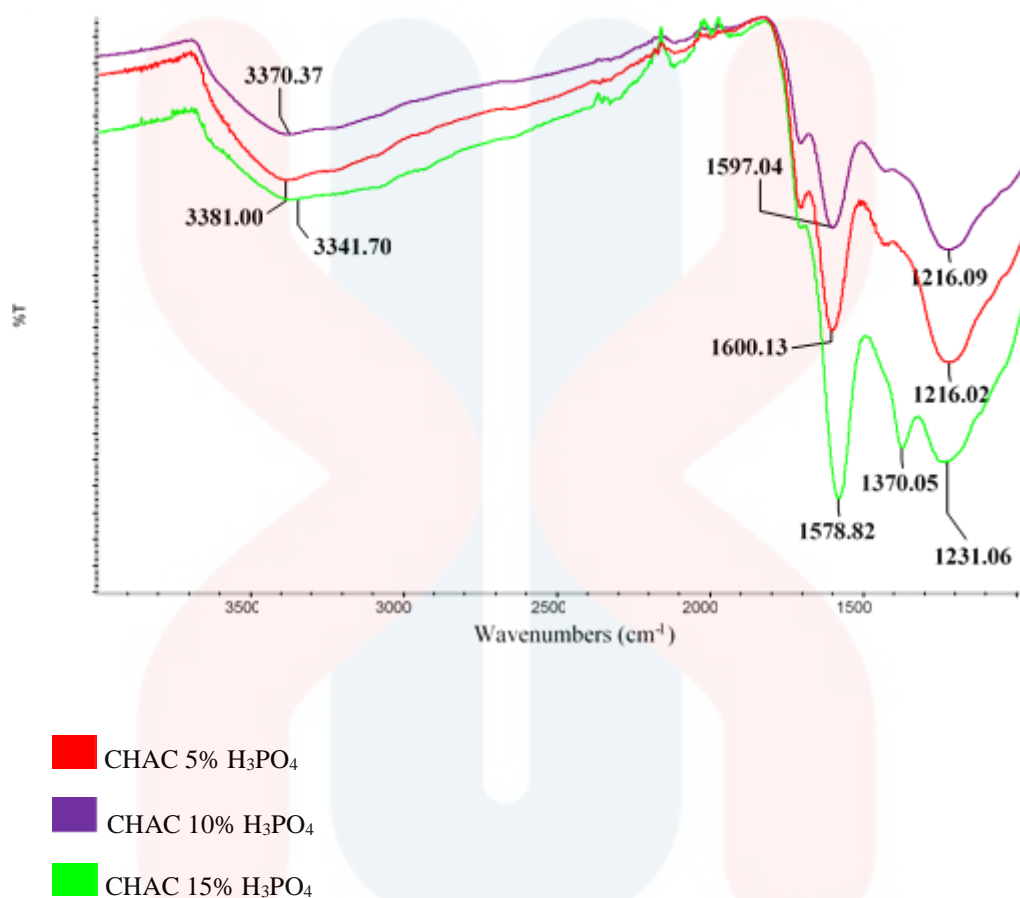


Figure 4.14: FTIR (ATR) spectra of coconut husks activated carbon (CHAC)

**Figure 4.14** above shows the interpretation of FTIR (ATR) spectral analysis for CHAC 5% H<sub>3</sub>PO<sub>4</sub>, CHAC 10% H<sub>3</sub>PO<sub>4</sub> and CHAC 15% H<sub>3</sub>PO<sub>4</sub>. From *CHAC 5% H<sub>3</sub>PO<sub>4</sub>* and *CHAC 10% H<sub>3</sub>PO<sub>4</sub>*, it was indicated that peaks 3381.00 cm<sup>-1</sup> and 1600.13 cm<sup>-1</sup> for *CHAC 5% H<sub>3</sub>PO<sub>4</sub>* and 3370.37 cm<sup>-1</sup> and 1597.04 cm<sup>-1</sup> for *CHAC 10% H<sub>3</sub>PO<sub>4</sub>* contributed to the aliphatic primary amines. This functional group consists of three (3) distinct classifications, which were primary, secondary and tertiary. Here, it appeared as primary amines, which correlated, to the number of groups attached to the nitrogen atom. The structural formula correlated to the functional group was represent



in Figure 4.15 below. NH peak also indicated the significant roles of amines group (Bello & Ahmad, 2012).

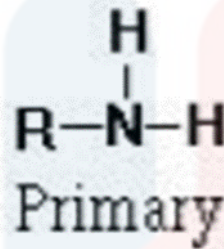


Figure 4.15: Structural formula for aliphatic primary amines

The last peak at  $1216.02 \text{ cm}^{-1}$  for *CHAC 5% H<sub>3</sub>PO<sub>4</sub>* and  $1216.09 \text{ cm}^{-1}$  for *CHAC 10% H<sub>3</sub>PO<sub>4</sub>* contributed to the functional group inorganic nitrites which consists of two (2) bands, around  $1260 \text{ cm}^{-1}$  which appeared as strong band and sharp and medium intensity band around  $825 \text{ cm}^{-1}$  as shown in Figure 4.16 below. CO stretching adsorption of carboxylic acid and alcohol was also detected at peaks range  $1250 \text{ cm}^{-1}$  to  $1000 \text{ cm}^{-1}$  (Fong, 2014). Figure 4.16 below shows the structural formula corresponding to the peaks respectively.

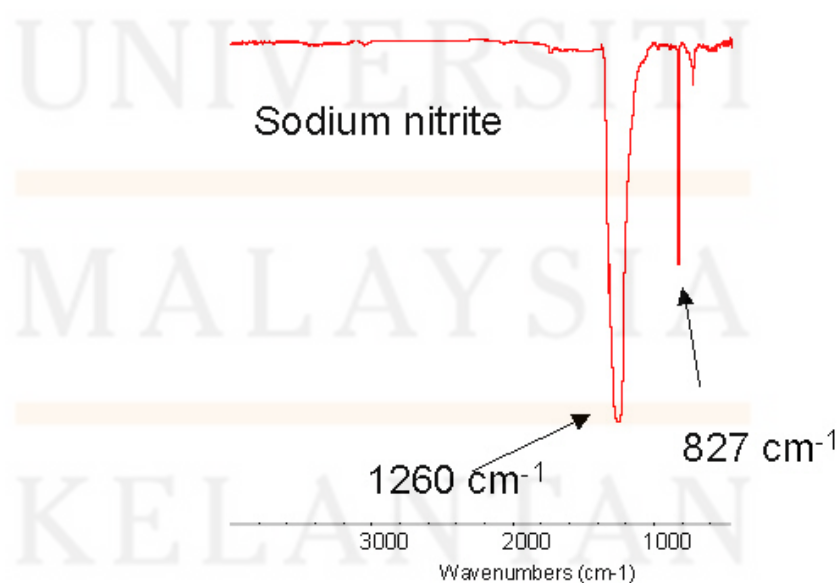


Figure 4.16: Structural formula for inorganic nitrites

The last sample of all contributed to the existence of aliphatic carboxylic acid salts at several peaks at **CHAC 15% H<sub>3</sub>PO<sub>4</sub>** include 3341.70 cm<sup>-1</sup>, 1578.82 cm<sup>-1</sup>, 1370.05 cm<sup>-1</sup> and 1231.06 cm<sup>-1</sup>. All peaks shows the same functional group where the existence of carboxylic acid by CO<sub>2</sub> stretching occurred due to the impregnation of NaOH to the CHAC.

## 4.5 Phase Identification of XRD Analysis

### 4.5.1 Phase Identification using XRD for Banana Peel Activated Carbon Impregnated with NaOH

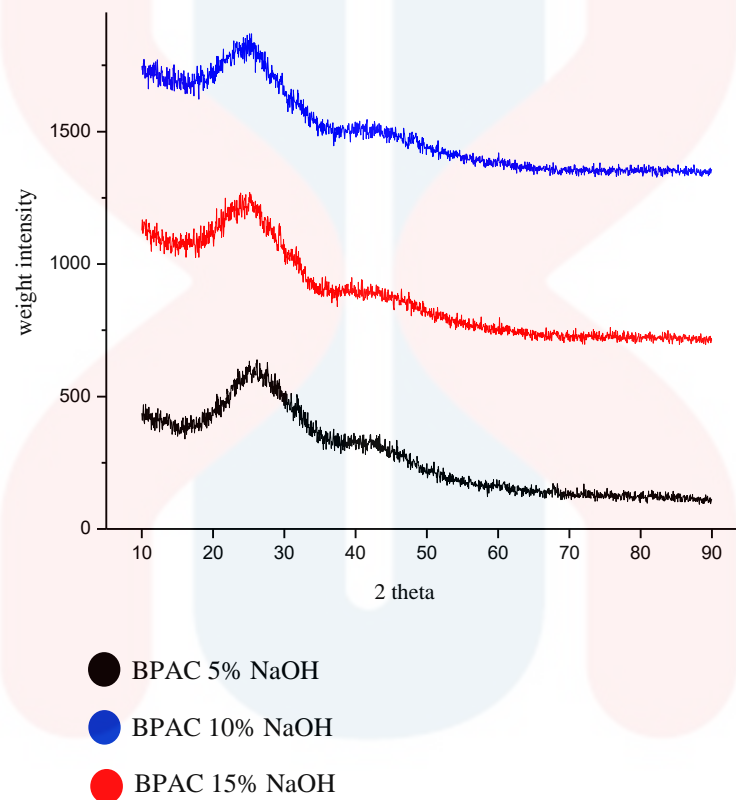


Figure 4.17: XRD pattern of banana peel activated carbon (BPAC) impregnated with NaOH

**Figure 4.17** above shows the result for XRD analysis for BPAC impregnated with 5%, 10% and 15% NaOH solution. They were termed as BPAC 5% NaOH, BPAC 10% NaOH and BPAC 15% NaOH respectively. BPAC 5% NaOH represents the peaks revealed the highest at angle 10°, 25° and 45° revealed the crystallinity of the samples was not too much. As it can be seen from the graph above, all three (3) samples shared the same peak angle that are 10°, 25° and 45° indicated lower crystallinity in the samples

analyzed. For BPAC 5% NaOH, the percentage crystallinity is 19.5% and amorphous is 80.5% while for BPAC 10% NaOH and BPAC 15% NaOH, both contributed to the same percentage crystallinity that are, 30.8% for crystallinity and 69.2% amorphous. This statement proved by Liu *et al.*, (2014) where it said, the strong and broad diffraction peaks of  $2\theta \approx 20^\circ$  and  $26^\circ$  assigned the amorphism.

#### 4.5.2 Phase Identification using XRD for Coconut Husks Activated Carbon Impregnated with NaOH

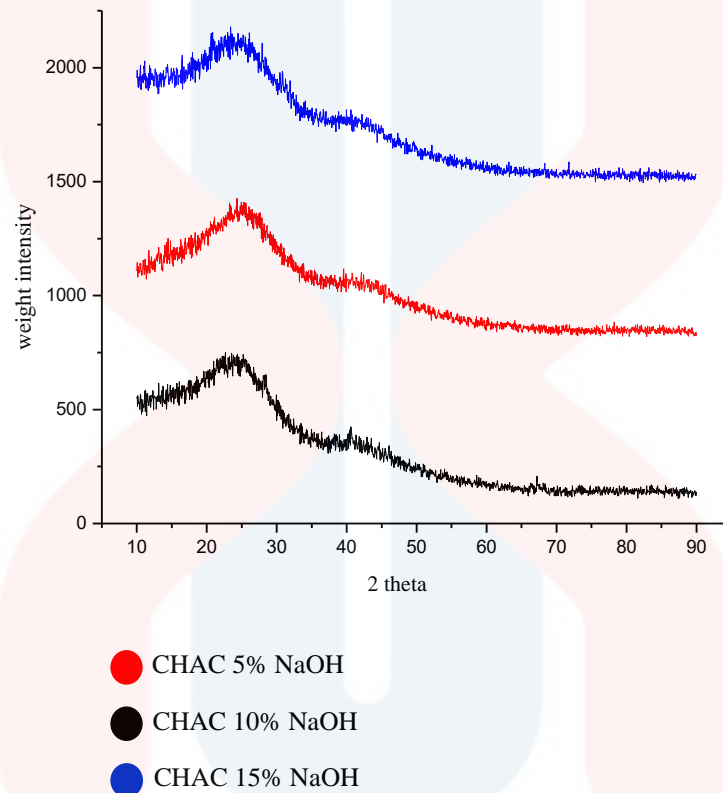


Figure 4.18: XRD pattern of coconut husks activated carbon (CHAC) impregnated with NaOH

**Figure 4.18** shows the CHAC impregnated with NaOH for CHAC 5% NaOH, CHAC 10% NaOH and CHAC 15% NaOH respectively where the broad peaks exist at angle  $11^\circ$ ,  $25^\circ$  and  $42^\circ$  respectively. Basically the broad peaks showed at angle  $24^\circ$  and  $42^\circ$  were said to have amorphous structure of AC (Taylor *et al.*, 2015). For CHAC 5% NaOH, the percentage crystallinity is 20.7% while amorphous is 79.3%. CHAC 10% NaOH showed 14.9% crystallinity and 85.1% amorphous. While the last sample, CHAC 15% NaOH showed 18.7% crystallinity and 81.3% amorphous.

### 4.5.3 Phase Identification using XRD Banana Peel Activated Carbon Impregnated with $H_3PO_4$

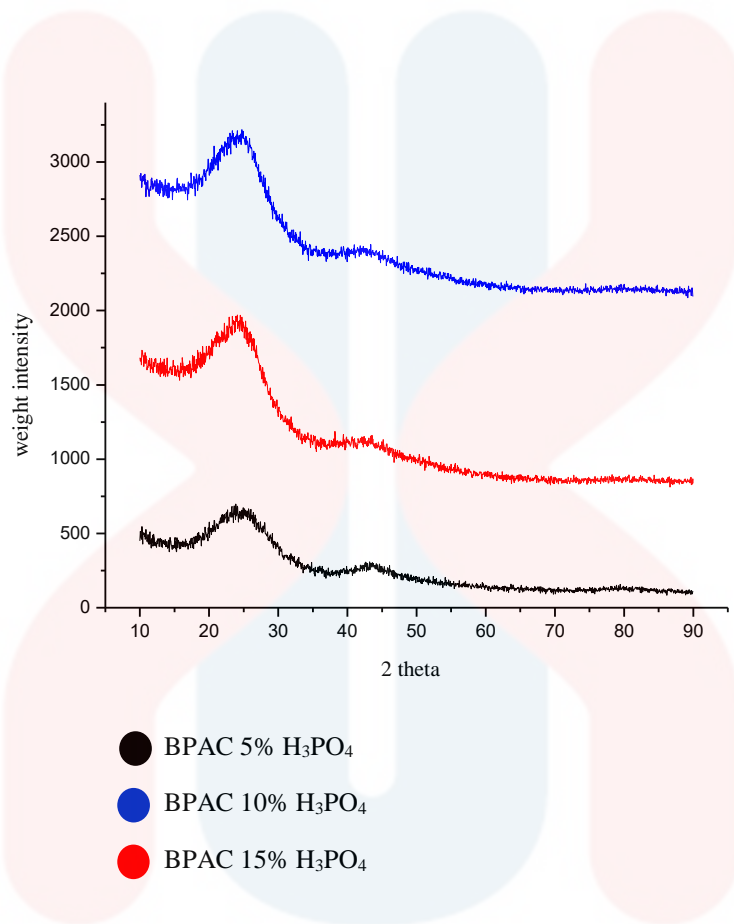


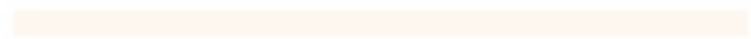
Figure 4.19: XRD pattern of banana peel activated carbon (BPAC) impregnated with  $H_3PO_4$

The highest peaks was detected at angle  $10^\circ$ ,  $25^\circ$  and  $44^\circ$  respectively indicated the amorphism of these samples where the broad and strong peak appeared to be in angle range  $24^\circ$  and  $42^\circ$  (Liu *et al.*, 2014). **Figure 4.19** showed the crystallinity of BPAC 5%  $H_3PO_4$  is 23.5% and the percentage amorphous is 76.5%. While for BPAC 10%  $H_3PO_4$ , percentage crystalline is 40.8% and amorphous is 59.2%. For BPAC 15%  $H_3PO_4$ , the percentage crystalline is 37.1% and amorphous is 62.9%. The percentages indicated that

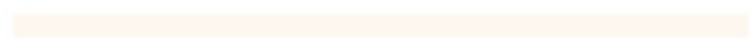
the AC produced was in amorphism state corresponding to the expected outcome above.



UNIVERSITI



MALAYSIA



KELANTAN

#### 4.5.4 Phase Identification using XRD Coconut Husks Activated Carbon Impregnated with $H_3PO_4$

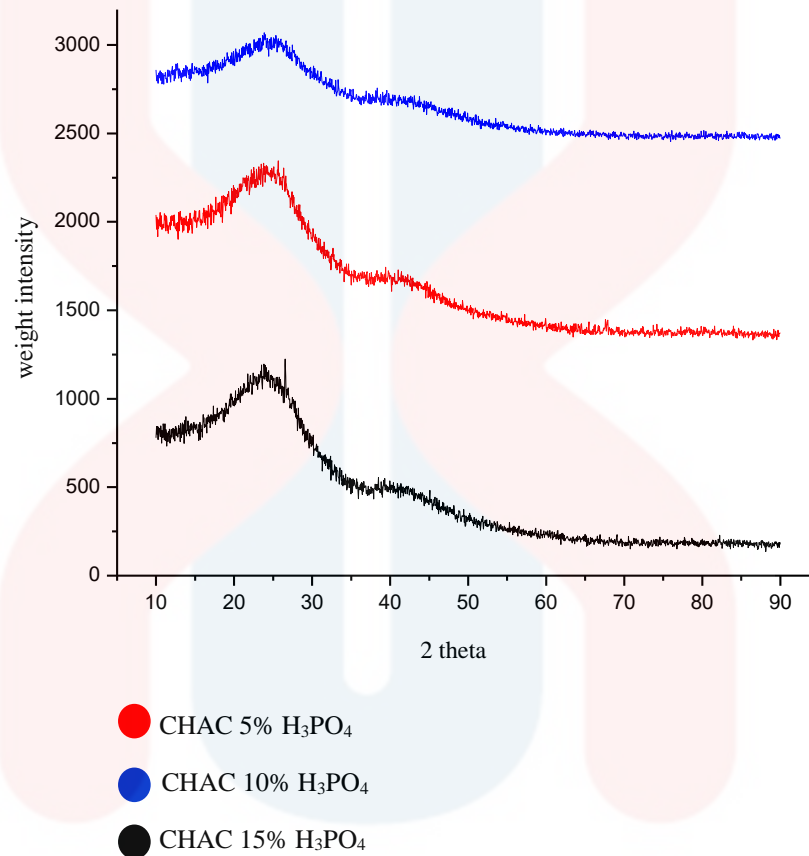


Figure 4.20: XRD pattern of coconut husks activated carbon (CHAC) impregnated with  $H_3PO_4$

**Figure 4.20** above shows the CHAC impregnated with 5%, 10% and 15%  $H_3PO_4$ . For CHAC 5%  $H_3PO_4$ , the percentage crystalline is 24.8% and percentage amorphous is 75.2%. CHAC 10%  $H_3PO_4$  showed percentage crystalline 27.6% and percentage amorphous 72.4% while for CHAC 15%  $H_3PO_4$  showed percentage crystallinity 16.0% and percentage amorphous 84.0%. Taylor *et al.*, (2015) said that amorphism of AC was around angle  $24^\circ$  and  $42^\circ$ .



## CHAPTER 5

### CONCLUSION

#### 5.1 Conclusion

This study showed that *Cocos Nucifera L.* (coconut) husks and *Musa Paradisiaca* (banana) peel were synthesized and characterized using two (2) distinct chemicals, which were Sodium Hydroxide (NaOH) and Phosphoric Acid (H<sub>3</sub>PO<sub>4</sub>). From this study, the results showed that activation process using H<sub>3</sub>PO<sub>4</sub> was better than NaOH because of the act of the modifying agents that triggered more porosity and surface area. The production of AC from waste materials lowered the cost and save energy. FTIR (ATR) and XRD analysis were applied in this study which gave the following results. For FTIR (ATR), the results showed the necessary functional group alcohol at peak around  $\approx 3000 \text{ cm}^{-1}$  and for XRD it was proved that the AC was in region amorphism because the peak appeared broad and strong at angle 20° and 42°.

#### 5.2 Recommendation

In future study, I suggest this study can be improved by adding analysis for this study using Brunauer, Emmett and Teller (BET) and Scanning Electron Microscopy (SEM). This can be utilized for the analysis of the surface area and the morphology of AC.

## REFERENCES

- Ali, A., & Saeed, K. (2015). Desalination and Water Treatment Phenol removal from aqueous medium using chemically modified banana peels as low-cost adsorbent, (May), 37–41.
- Azmi, N. A. I., Zainudin, N. F., Ali, U. F. M., & Senusi, F. (2015). Adsorption kinetics on basic red 46 removal using Cerbera odollam activated carbon. *Journal of Engineering Science and Technology*, 10(Spec.issue5), 82–91.
- Bello, O. S., & Ahmad, M. A. (2012). Coconut ( *Cocos nucifera* ) Shell Based Activated Carbon for the Removal of Malachite Green Dye from Aqueous Solutions. *Separation Science and Technology*, 47(6), 903–912.
- Chandra, T. C., Mirna, M. M., Sunarso, J., Sudaryanto, Y., & Ismadji, S. (2009). Activated carbon from durian shell: Preparation and characterization. *Journal of the Taiwan Institute of Chemical Engineers*, 40(4), 457–462.
- Cobb, A., Warms, M., Maurer, E. P., & Chiesa, S. (2012). Low-Tech Coconut Shell Activated Charcoal Production. *International Journal for Service Learning in Engineering*, 7(1), 93–104.
- Duran-Valle, C. J. (2015). Technique Employed in the Physicochemical Characterization of Activated Carbon. In A. Brooks (Ed.), *Waste Water Treatment Activated Carbon and Other Methods* (p. 92).
- Fong, M. (2014). Treatment and decolorization of biologically treated Palm Oil Mill Effluent ( POME ) using banana peel as novel biosorbent, 132, 237–249.
- Getachew, T., Hussen, A., & Rao, V. M. (2014). Defluoridation of water by activated carbon prepared from banana ( *Musa paradisiaca* ) peel and coffee ( *Coffea arabica* ) husk.
- Gratisito, M. K. B., Panyathanmaporn, T., Chumnanklang, R. A., Sirinuntawittaya, N., & Dutta, A. (2008). Production of activated carbon from coconut shell: Optimization using response surface methodology. *Bioresource Technology*, 99(11), 4887–4895.
- I, I. A., O, I. A., & I, B. H. (2012). Comparison of the Adsorptive Capacity of Raw Materials in Making Activated Carbon Filter for Purification of Polluted Water for Drinking, 2(9), 754–760.
- Inegbenebor, A. I., Inegbenebor, A. O., & Boyo, H. I. (2012). Comparison of the Adsorptive Capacity of Raw Materials in Making Activated Carbon Filter for Purification of Polluted Water for Drinking. *ARNP Journal of Science and Technology*, 2(9), 754–760. Retrieved from <http://covenantuniversity.edu.ng/Profiles/Inegbenebor-Anthony/Comparison-Of-The-Adsorptive-Capacity-Of-Raw-Materials-In-Making-Activated-Carbon-Filter-For-Purification-Of-Polluted-Water-For-Drinking>
- Ketcha, J. M., Dina, D. J. D., Ngomo, H. M., & Ndi, N. J. (2012). Preparation and Characterization of Activated Carbons Obtained from Maize Cobs by Zinc Chloride Activation, 2(4), 136–160.
- Laginhas, C., Nabais, J. M. V., & Titirici, M. M. (2016). AC SC. *Microporous and Mesoporous Materials*.

- Latinwo, G. K., & Agarry, S. E. (2015). Removal of Phenol from Paint Wastewater by Adsorption onto Phosphoric Acid Activated Carbon Produced from Coconut Shell : Isothermal and Kinetic Modelling Studies, 7(5), 123–138.
- Lemaro Fereiti Angelo, R. B. K. (2012). University of Nairobi, (May).
- Li, W., Yang, K., Peng, J., Zhang, L., Guo, S., & Xia, H. (2008). Effects of carbonization temperatures on characteristics of porosity in coconut shell chars and activated carbons derived from carbonized coconut shell chars, 8, 190–198.
- Liu, R., Yin, F., Zhang, J., & Zhang, Z. (2014). RSC Advances chemically modified banana peel for size-selective.
- Ma, J., Huang, D., & Zou, J. (2014). Adsorption of methylene blue and Orange II pollutants on activated carbon prepared from banana peel.
- Mahanim, S., Asma, I. W., Rafidah, J., Puad, E., & Shaharuddin, H. (2011). Production of Activated Carbon From Industrial Bamboo Wastes, 23(4), 417–424.
- Nowicki, P., Kazmierczak, J., & Pietrzak, R. (2015). Comparison of physicochemical and sorption properties of activated carbons prepared by physical and chemical activation of cherry stones. *Powder Technology*, 269, 312–319.
- Pathak, P. D., Mandavgane, S. A., & Kulkarni, B. D. (2015). Fruit peel waste as a novel low-cost bio adsorbent, 31(4), 361–381.
- Pradhan, S. (2011). *Production and characterization of Activated Carbon produced from a suitable Industrial sludge Department of Chemical Engineering.*
- Roopan, S. M., & Elango, G. (2015). Exploitation of Cocos nucifera a non-food toward the biological and nanobiotechnology field. *Industrial Crops and Products*, 67, 130–136.
- Selvanathan, N., & Subki, N. S. (2015). Dye Adsorbent By Pineapple Activated Carbon : H<sub>3</sub>PO<sub>4</sub> AND NaOH ACTIVATION, 10(20), 9476–9480.
- Shankar, P. A. (2008). Coconut Shell Based Activated Carbon with No Green House Gas Emission.
- Taylor, P., Gupta, H., & Gupta, B. (2015). Desalination and Water Treatment Adsorption of polycyclic aromatic hydrocarbons on banana peel activated carbon, (April), 37–41.
- Taylor, P., Pathak, P. D., Mandavgane, S. A., & Kulkarni, B. D. (n.d.). Desalination and Water Treatment Utilization of banana peel for the removal of benzoic and salicylic acid from aqueous solutions and its potential reuse, (June 2015), 37–41.
- Thomas, B. N., George, S. C., & Shell, C. O. (2015). iMedPub Journals Production of Activated Carbon from Natural Sources Abstract Trends in Green Chemistry Preparation of Activated Carbon from Preparation of Activated Carbon from Bamboo Chips Preparation of Activated Carbon from Cherry Stones, 1–5.
- Virginia Hernandez-Montoya, J. G.-S. and J. I. B.-L. (2015a). Thermal Treatment and Activation Procedures Used in the Preparation of Activated Carbon. In A. Brooks (Ed.), *Waste Water Treatment Activated Carbon and Other Methods* (p.

92).

Virginia Hernandez-Montoya, J. G.-S. and J. I. B.-L. (2015b). *Waste Water Treatment Activated Carbon and Other Methods*. (A. Brooks, Ed.).

Yusufu, M. I., Ariaahu, C. C., & Igbabul, B. D. (2012). Production and characterization of activated carbon from selected local raw materials, 6(9), 123–131.

Zheng, H., & Wang, L. (2013). Banana Peel Carbon Containing Functional Groups Applied to the Selective Adsorption of Au ( III ) from Waste Printed Circuit Boards, 2013(April), 29–36.